

## RESEARCH ARTICLE

## Resident bacteria contribute to opportunistic infections of the respiratory tract

Yifan Wu<sup>1</sup>, Yongqiang Wang<sup>2</sup>, Huiming Yang<sup>2</sup>, Qian Li<sup>1</sup>, Xiaoxia Gong<sup>1</sup>, Guozhong Zhang<sup>2\*</sup>, Kui Zhu<sup>1,3\*</sup>

**1** National Center for Veterinary Drug Safety Evaluation, College of Veterinary Medicine, China Agricultural University, Beijing, China, **2** Key Laboratory of Animal Epidemiology of the Ministry of Agriculture, College of Veterinary Medicine, China Agricultural University, Beijing, China, **3** Beijing Key Laboratory of Detection Technology for Animal-Derived Food Safety and Beijing Laboratory for Food Quality and Safety, China Agricultural University, Beijing, China

☯ These authors contributed equally to this work.

\* [zhanggz@cau.edu.cn](mailto:zhanggz@cau.edu.cn) (GZ); [zhuk@cau.edu.cn](mailto:zhuk@cau.edu.cn) (KZ)



## OPEN ACCESS

**Citation:** Wu Y, Wang Y, Yang H, Li Q, Gong X, Zhang G, et al. (2021) Resident bacteria contribute to opportunistic infections of the respiratory tract. *PLoS Pathog* 17(3): e1009436. <https://doi.org/10.1371/journal.ppat.1009436>

**Editor:** Andreas Peschel, University of Tübingen, GERMANY

**Received:** August 7, 2020

**Accepted:** March 1, 2021

**Published:** March 19, 2021

**Copyright:** © 2021 Wu et al. This is an open access article distributed under the terms of the [Creative Commons Attribution License](https://creativecommons.org/licenses/by/4.0/), which permits unrestricted use, distribution, and reproduction in any medium, provided the original author and source are credited.

**Data Availability Statement:** All relevant data are within the paper and its [Supporting Information](#) files. All WGS files are available from the NCBI database (accession numbers PRJNA648655, PRJNA648661). All bacterial community files are available from the NCBI database (accession number PRJNA646660).

**Funding:** The work was supported by the National Key Research and Development Program of China (2018YFD0500106, G.Z.) and National Natural Science Foundation of China (31922083, K.Z.). The funders had no role in study design, data collection

## Abstract

Opportunistic pathogens frequently cause volatile infections in hosts with compromised immune systems or a disrupted normal microbiota. The commensalism of diverse microorganisms contributes to colonization resistance, which prevents the expansion of opportunistic pathogens. Following microbiota disruption, pathogens promptly adapt to altered niches and obtain growth advantages. Nevertheless, whether and how resident bacteria modulate the growth dynamics of invasive pathogens and the eventual outcome of such infections are still unclear. Here, we utilized birds as a model animal and observed a resident bacterium exacerbating the invasion of *Avibacterium paragallinarum* (previously *Haemophilus paragallinarum*) in the respiratory tract. We first found that negligibly abundant *Staphylococcus chromogenes*, rather than *Staphylococcus aureus*, played a dominant role in *Av. paragallinarum*-associated infectious coryza in poultry based on epidemic investigations and *in vitro* analyses. Furthermore, we determined that *S. chromogenes* not only directly provides the necessary nutrition factor nicotinamide adenine dinucleotide (NAD<sup>+</sup>) but also accelerates its biosynthesis and release from host cells to promote the survival and growth of *Av. paragallinarum*. Last, we successfully intervened in *Av. paragallinarum*-associated infections in animal models using antibiotics that specifically target *S. chromogenes*. Our findings show that opportunistic pathogens can hijack commensal bacteria to initiate infection and expansion and suggest a new paradigm to ameliorate opportunistic infections by modulating the dynamics of resident bacteria.

## Author summary

There is an urgent need for novel intervention strategies and techniques to address the increasing dissemination of multidrug-resistant Gram-negative bacterial pathogens. More importantly, secondary bacterial infections are common in clinical practice, whereas the growth dynamics of each individual in such coinfections are still complicated and elusive.

and analysis, decision to publish, or preparation of the manuscript.

**Competing interests:** The authors have declared that no competing interests exist.

In the current study, we first identified *Staphylococcus* spp., especially negligibly abundant *S. chromogenes*, facilitating the pathogenesis of *Av. paragallinarum*, a Gram-negative bacterium responsible for severe and acute avian respiratory disease worldwide. Furthermore, we developed therapeutic strategies using specific antibiotics against *Staphylococcus* spp. to relieve clinical symptoms and reduce *Av. paragallinarum*-associated infections in chickens. These results show that implementation of a proper intervention strategy can prevent opportunistic infections by regulating the microbiota and elucidate the development of alternative approaches for treating Gram-negative pathogenic bacterial infections.

## Introduction

Microbial communities coevolved with hosts are abundant on the surface of their bodies and the respiratory and gastrointestinal tracts. The communities consist of trillions of commensal microorganisms, also termed the microbiota, periodically interacting with various pathogenic invaders. Although resident bacteria in the mucosa are necessary to hosts to exclude exogenous pathogens [1, 2], they may be exploited by pathogens to impair hosts under certain circumstances. For instance, *Bacteroides* species, comprising a predominant genus in the intestinal tract, promote the replication and expression of virulence genes of *Escherichia coli* [3, 4]. Additionally, *Staphylococcus aureus* can prevent clearance by macrophages through the secretion of  $\alpha$ -toxin, resulting in the expansion of opportunistic pathogens [5]. Similarly, collateral damage to the intestinal microbiota by oral antibiotics and invasive viruses renders hosts susceptible to *Clostridium difficile* [6] and *Haemophilus* spp. [7], respectively. Similar to the well-characterized modulation of bacterial dynamics in the gut, we suspected that opportunistic bacteria might also utilize resident bacteria to initiate colonization and invasion in the respiratory tract.

In contrast to the presence of abundant nutrients in the intestinal tract, resident bacteria in the respiratory tract commonly suffer from a shortage of energy sources in healthy individuals [8], especially microorganisms such as *Haemophilus* spp. that require rich nutrition. *Haemophilus* spp. are commensal Gram-negative bacteria in both humans and animals, serving as opportunistic pathogens for volatile diseases [9, 10]. Normally, the abundance of  $\text{NAD}^+$  in the respiratory tract of healthy individuals is insufficient for their survival and growth [11–13] because the limited resource of  $\text{NAD}^+$  is subtly modulated by hosts to maintain homeostasis [13, 14]. Hence, we hypothesized that the increased level of  $\text{NAD}^+$  is a prerequisite for the subsequent infections associated with *Haemophilus* spp. Despite the structural anatomical differences between mammals and birds, similar syndromes and potential bird-borne zoonoses have been described [15–20]. Therefore, it is convenient to employ birds to explore the contribution of resident bacteria to such infections. Infectious coryza (IC) is an acute respiratory infection of poultry worldwide caused by *Avibacterium paragallinarum*, previously known as *Haemophilus paragallinarum*, with subsequent consequences, including poor growth performance of growing chickens and a remarkable decrease in egg production (reduced by 10%–40%) [21, 22]. Interestingly, the principle of the satellitism test has been utilized for decades to isolate and identify infections associated with *Haemophilus* spp. and *Av. paragallinarum* [23]. Nevertheless, it is still unknown whether and how *Staphylococcus* spp. contribute to the pathogenesis of such infections *in vivo*.

In the present work, we observed negligibly abundant *Staphylococcus chromogenes* directly facilitating the survival of *Av. paragallinarum* in the upper respiratory tract (URT) of chickens.

In addition, host cells in the presence of *S. chromogenes* and *Av. paragallinarum* were forced to increase the synthesis and release of NAD<sup>+</sup>, which in turn promoted the replication of *Av. paragallinarum*. In addition, antimicrobial agents targeting *S. chromogenes* significantly relieved clinical symptoms and reduced the burden of *Av. paragallinarum* in chickens. Our results indicate that resident bacteria in the respiratory tract can promote the invasion and replication of opportunistic pathogens, and modulation of commensal bacterial dynamics may be an alternative strategy to prevent and control such infections.

## Results

### Extensive spread of multi-drug resistant *Av. paragallinarum* in China

To investigate persistent *Haemophilus* infection in the respiratory tract of birds, we first launched an epidemiological investigation by online questionnaires to reveal the prevalence of IC. We found that the rate of IC outbreaks was 59.2% (61/103) in poultry farms from 11 provinces in China (S1 Fig), which was highly associated with the breeds and origins of growing birds (S1 and S2 Tables). Additionally, we observed that the implementation of vaccinations was not able to provide enough protection against *Av. paragallinarum* infection. Therefore, we collected samples of the nasal cavity and infraorbital sinuses from 20 birds with clinical signs of IC (Fig 1A) because *Av. paragallinarum* commonly colonize such anatomic interconnected sites [21, 24]. In total, we obtained 173 isolates from 20 birds, of which 10.4% (18) were *Av. paragallinarum*. One isolate belonged to the type serovar B, two isolates were not typeable, and the other 15 isolates were serovar C based on the DNA sequence homology of the outer membrane protein HMTp210 (S2A Fig) [25]. However, previous reports show that *Av. paragallinarum* serovars A and B are dominant in China [26, 27]. Subsequently, these 18 *Av. paragallinarum* isolates were divided approximately into two clusters according to core-genome SNP-based phylogenetic trees (S2A Fig). Notably, *Staphylococcus* was the most prevalent genus in the other isolates, accounting for 23.87% (37/155), among which *S. chromogenes* displayed the highest proportion (67.57%, 25/37) (Fig 1B). Furthermore, we found that 94.6% (35/37) of *Staphylococcus* isolates were coagulase-negative *Staphylococcus* (CoNS) (Fig 1B), consistent with the phenomenon that many CoNS are associated with chronic rhinosinusitis [28]. Last, most *Av. paragallinarum* and *S. chromogenes* phenotypically showed multidrug resistance through whole-genome sequencing and antimicrobial susceptibility tests (S4 and S5 Tables and S4A and S4B Fig).

To better understand the contribution of resident bacteria to *Haemophilus*-associated infections, we performed further analyses based on custom synergistic indexes, including the rates of isolation and colocalization and the radii of satellitism on blood agar plates (Fig 1C and 1D). Two *Av. paragallinarum* isolates were randomly selected for satellitism tests, and the radii were measured after 48 h (Figs 1C, 1D and S3A and S3B and S3B). We observed that most bacteria in the *Staphylococcus* genus, particularly *S. chromogenes*, promoted the growth of *Av. paragallinarum* (S3 Table). Altogether, these results suggest that *S. chromogenes* probably facilitates *Av. paragallinarum* infection in the respiratory tract due to the high isolation rate, colocalization rate and positive satellitism phenotype.

To dissect the interaction between *Av. paragallinarum* and *S. chromogenes*, we characterized the virulence genes of both *Av. paragallinarum* and *S. chromogenes* based on whole-genome sequencing. Genes encoding type IV pili (*piliA*, *piliB* and *piliQ*) and exopolysaccharides (*pgi*, *manA*, *manB*, *mrsA*, *galE* and *galU*) were detected in *Av. paragallinarum* compared to other *Haemophilus* isolates (S5A Fig). Moreover, we detected the presence of genes responsible for cell adhesion and immune evasion in these *S. chromogenes* isolates, including *atl*, *capO*, *capD*, *adsA* and *sbi*. Notably, genes encoding toxins, such as beta hemolysin (*hlyB*), lipases

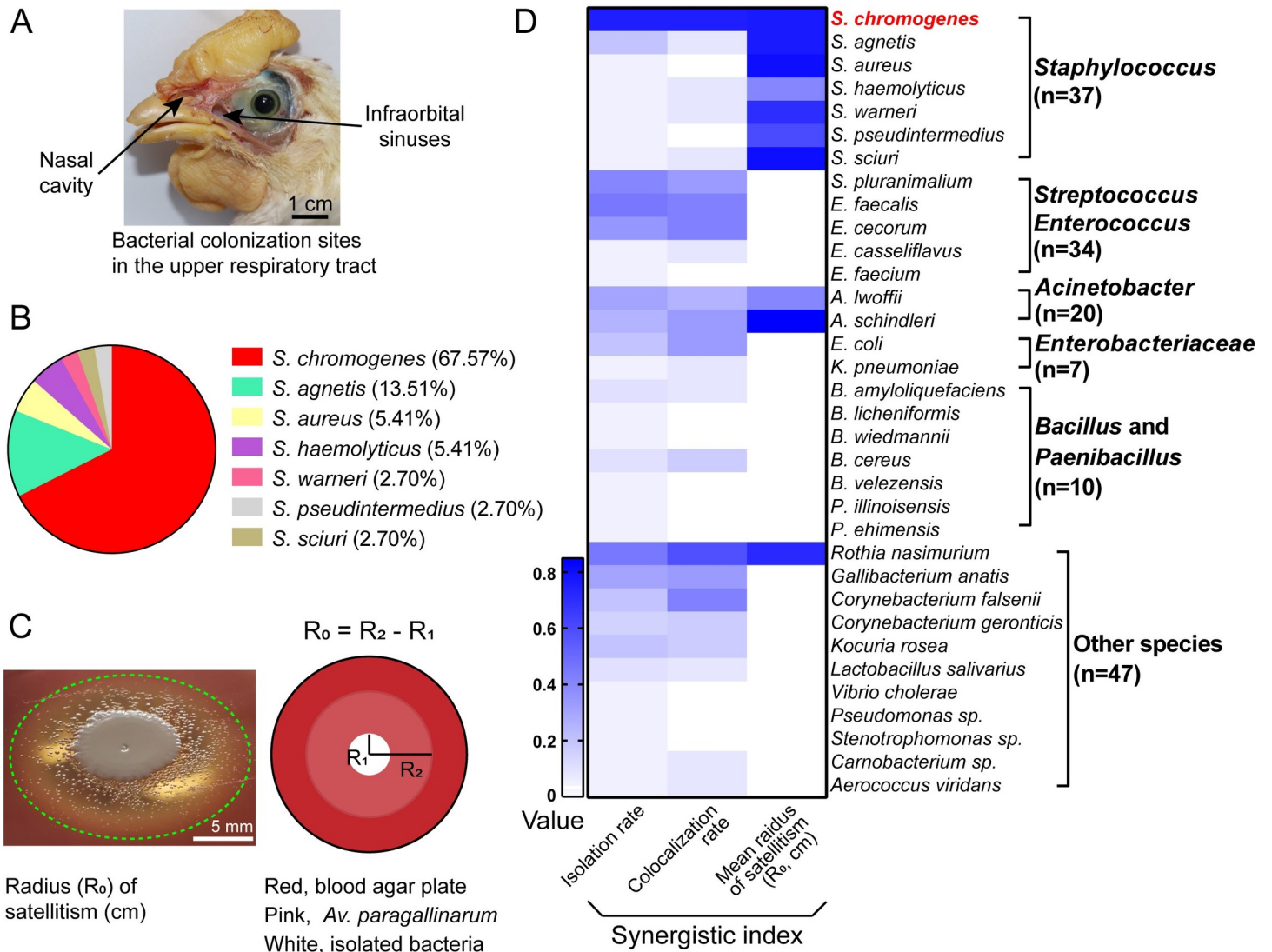


**Fig 1. *S. chromogenes* is closely related to *Av. paragallinarum* infection.** (A) Bacterial samples were collected from the nasal cavity and infraorbital sinuses of 20 birds with clinical symptoms. (B) Distribution of *Staphylococcus* spp. (C) Representative image of the satellitism of *Av. paragallinarum* on blood agar plates after cocultivation for 48 h. (D) Custom synergistic indexes, including the isolation rates (0–1), colocalization rates (0–1), and the mean radii of satellitism (cm).

<https://doi.org/10.1371/journal.ppat.1009436.g001>

(*lip* and *geh*) and thermonuclease (*nuc*), were also confirmed (S5B Fig), which have been identified in *S. chromogenes*-mediated mastitis of bovines and goats [29, 30]. Taken together, our results indicate that both *S. chromogenes* and *Av. paragallinarum* isolated from the respiratory tract of birds are likely opportunistic pathogens with the potential to express diverse virulence factors.

### *S. chromogenes* directly facilitated the survival of *Haemophilus in vitro*

To estimate the connection between *S. chromogenes* and *Av. paragallinarum*, we first examined their growth rate using homemade broth media supplemented with different blood components (Fig 2A). We observed that *Av. paragallinarum* died gradually in the medium, and no living cells were detected after monoculture for 10 h. Conversely, both *Av. paragallinarum* and *S. chromogenes* survived in the coculture system (Fig 2B). To obtain a better understanding of

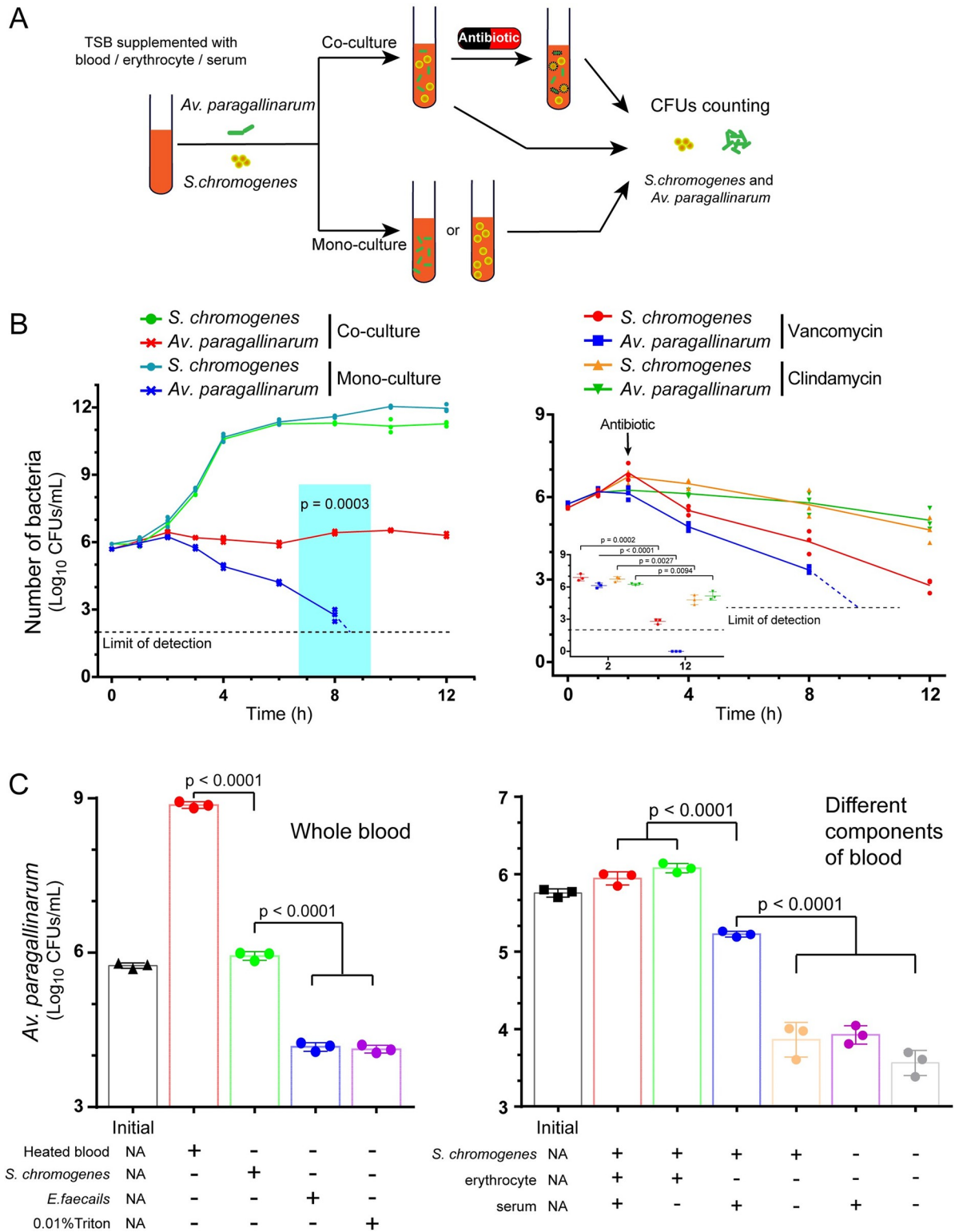


**Fig 2. *S. chromogenes* supports the survival of *Av. paragallinarum* in vitro.** (A) Workflow of *in vitro* coculture experiments. *S. chromogenes* SC10 and *Av. paragallinarum* X1-1S-1 were cocultured or monocultured in homemade broth media with or without antimicrobial agents. The CFUs/mL bacteria of all groups were subsequently calculated. (B) The growth dynamic of *S. chromogenes* and *Av. paragallinarum* in the presence of 5% (v/v) whole blood with (picture on the right) or without antimicrobial agents (picture on the left). LOD, limit of detection. *P* values were determined by unpaired *t*-test. The values of three biological replicates are shown as individual points

(n = 3). (C) Replication of *Av. paragallinarum* in the presence of whole blood or blood components. NA, not applicable. *P* values were determined by one-way ANOVA. The mean of three biological replicates is shown, and error bars represent the standard deviation (SD) (n = 3).

<https://doi.org/10.1371/journal.ppat.1009436.g002>

the role of *S. chromogenes*, we explored antibiotics (vancomycin and clindamycin) that specifically target Gram-positive bacteria in the coculture system. The number of *Av. paragallinarum* decreased rapidly in the presence of bactericidal vancomycin but remained constant under the treatment with bacteriostatic clindamycin (Figs 2B and S6A). These results imply that live *S. chromogenes* plays a crucial role in the maintenance and survival of *Av. paragallinarum*. Additionally, we tested other bacteria, such as *Enterococcus faecalis*, which also exhibited high rates of isolation and colocalization; however, we found no such potentiation to *Av. paragallinarum* (Fig 2C). Therefore, it seems that there is a unique interaction between *Av. paragallinarum* and *S. chromogenes*.

Interestingly, *Av. paragallinarum* grew well in tryptic soy broth (TSB) supplemented with heat-treated blood. Heating blood can not only inactivate NADase but also promote the release of intracellular NAD<sup>+</sup> to facilitate the growth of *Haemophilus* [31]. In contrast, blood cell lysis by Triton cannot support bacterial replication, although such surfactant is nontoxic to *Av. paragallinarum* (Figs 2C and S6A). To further understand the effect of *S. chromogenes*, we examined the survival of *Av. paragallinarum* in media supplemented with different blood components. Remarkably, *Av. paragallinarum* grew to high density in the presence of *S. chromogenes* together with either whole blood or erythrocytes (Fig 2C). These results suggest that the presence of *S. chromogenes* is a prerequisite for the survival of *Av. paragallinarum*. To extend our observation, we verified the interaction between *S. chromogenes* and *Haemophilus parasuis*, which typically causes Glässer's disease in pigs [32]. We confirmed that *H. parasuis* could not grow on blood agar in the absence of *S. chromogenes* (Fig 3A). Additionally, *S. chromogenes* significantly increased the number of *H. parasuis* in the medium supplemented with blood or serum (Fig 3B). Therefore, the promotional effect of *S. chromogenes* on the growth of *Haemophilus* spp. should be universal.

To investigate the underlying mechanism, we directly measured the NAD<sup>+</sup> content in the culture medium using a colorimetric assay [33]. The accumulation of NAD<sup>+</sup> reached its peak after culturing *S. chromogenes* for 4 h (Fig 4A). Interestingly, we found that the NAD<sup>+</sup> content in the supernatants of cultures of various *S. chromogenes* isolates exhibited similar levels (Fig 4B). Similarly, other species of *Staphylococcus* showed the capability to provide NAD<sup>+</sup> (Fig 4C). We observed that both the NAD<sup>+</sup> content and bacterial number increased when *S. chromogenes* was cultured at 42°C (Figs 4C and S7A and S7B), implying that *S. chromogenes* probably adapts to the body temperature of birds. Although the sole *Staphylococcus sciuri* isolate displayed high NAD<sup>+</sup> production, there was no difference in the growth of *Av. paragallinarum* when cocultured with either *S. chromogenes* or *S. sciuri* (S7C and S7D Fig). Collectively, our findings indicate that the prevailing *S. chromogenes* may dominantly provide sufficient NAD<sup>+</sup> for the survival of *Av. paragallinarum*.

### ***S. chromogenes* exacerbated the infection of *Av. paragallinarum***

Given that *S. chromogenes* promotes the survival of *Av. paragallinarum* *in vitro*, we next investigated the role of *S. chromogenes* in animal models. Briefly, six-week SPF birds were randomly divided into four groups with six birds in each group and challenged with *Av. paragallinarum* alone or accompanied by *S. chromogenes* sequentially. Moreover, vancomycin was applied not only to remove the intrinsically colonized *Staphylococcus* spp. but also to kill *S. chromogenes* after infection (Fig 5A). The birds coinfecting with *Av. paragallinarum* and *S. chromogenes*

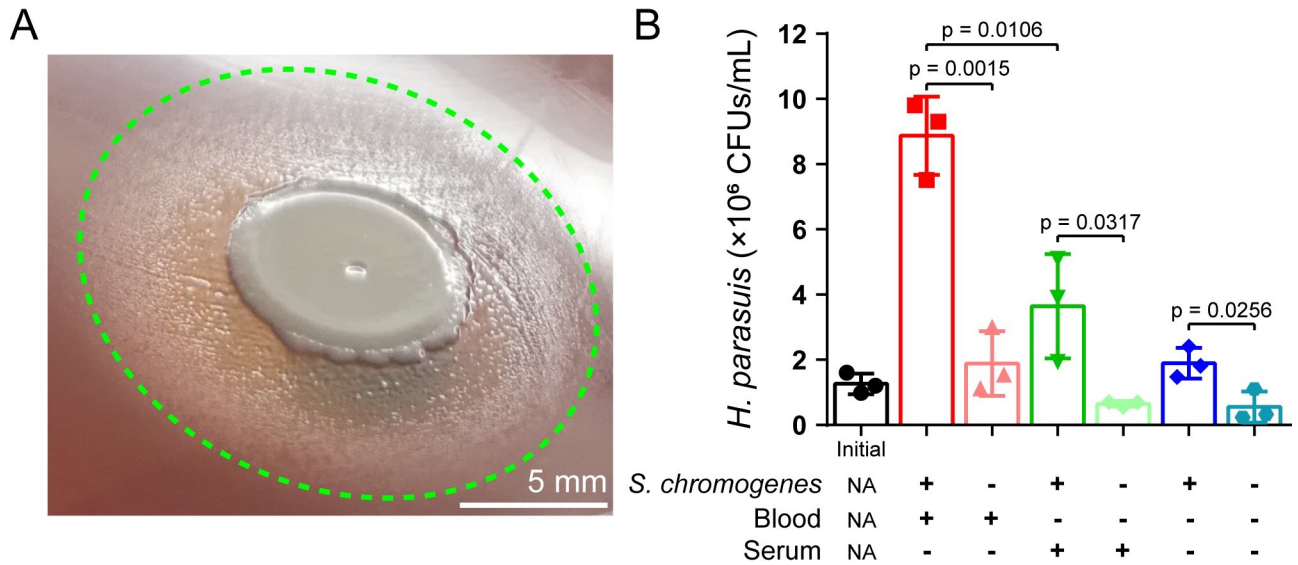


**Fig 3. *S. chromogenes* supports the growth of *H. parasuis* in vitro.** (A) Satellitism formed by *S. chromogenes* and *H. parasuis* after coculturing for 48 h. (B) *H. parasuis* displayed high density in the presence of *S. chromogenes*, together with either blood or serum. *H. parasuis* was monocultured or cocultured with *S. chromogenes* in TSB supplemented with different nutrients for 6 h. NA, not applicable. *P* values were determined by unpaired *t*-test. The mean of three biological replicates is shown, and error bars represent the standard deviation (SD) (*n* = 3).

<https://doi.org/10.1371/journal.ppat.1009436.g003>

showed more severe clinical symptoms than those infected with *Av. paragallinarum* alone (Figs 5B–5E and S8). Consistently, the burden of *Av. paragallinarum* in the nasal cavity and infraorbital sinuses increased approximately 100 times compared with the mono-infection (Fig 5F and 5G). Although the relative abundances of *Erwinia*, *Lactobacillus* and *Pseudomonas* increased (Fig 5G), none of them were isolated clinically (S3 Table). Remarkably, we observed

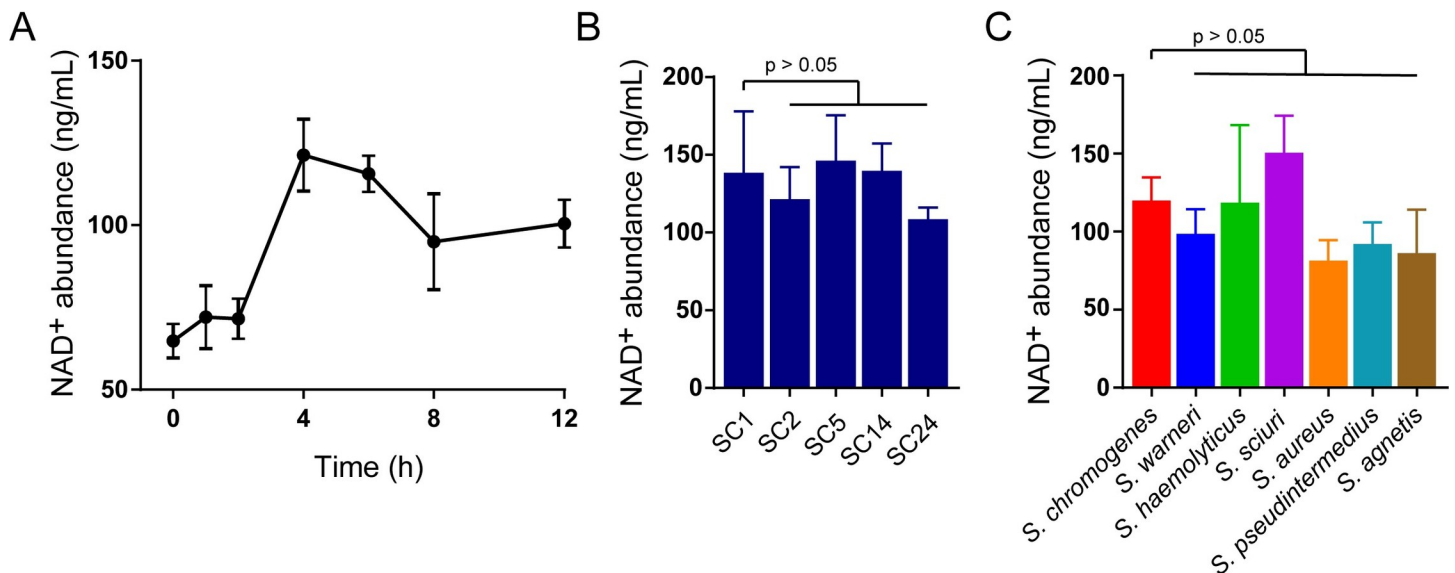


**Fig 4. Accumulation of *Staphylococcus*-derived NAD<sup>+</sup> promotes the survival of *Av. paragallinarum*.** (A) The NAD<sup>+</sup> content in the medium. *S. chromogenes* SC10 was monocultured in TSB supplemented with 5% (v/v) serum at 37°C. (B) NAD<sup>+</sup> content in cultures of five *S. chromogenes* isolates after 4 h. (C) NAD<sup>+</sup> content in cultures of different *Staphylococcus* isolates after 4 h at 37°C. *P* values were determined by one-way ANOVA. The mean of three biological replicates is shown, and error bars represent the standard deviation (SD) (*n* = 3).

<https://doi.org/10.1371/journal.ppat.1009436.g004>

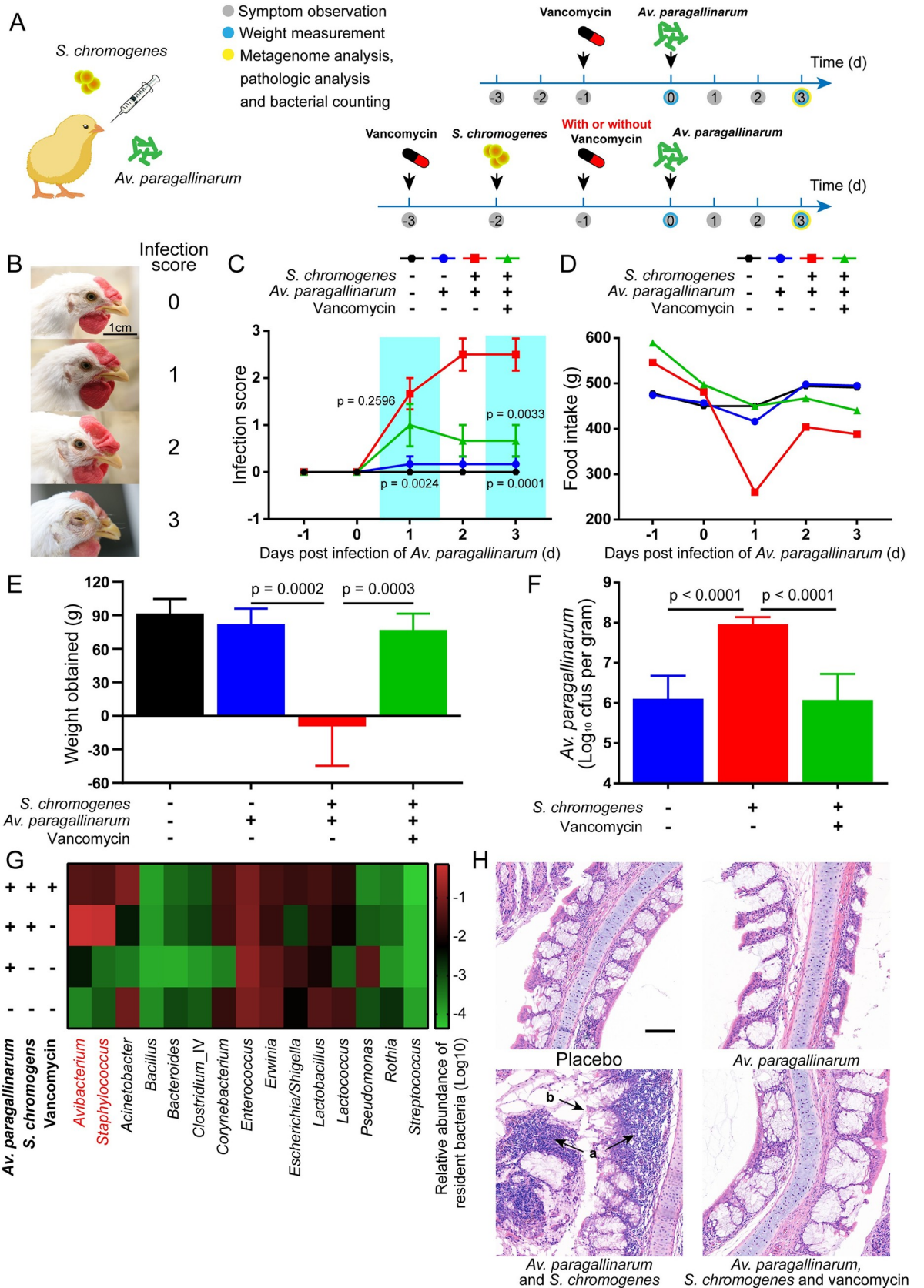


**Fig 5. *S. chromogenes* aggravates the infection of *Av. paragallinarum*.** (A) Scheme of animal models. SPF white leghorn chickens were randomly divided into four groups with six chickens in each group. Bacterial infection ( $10^9$  CFUs per bird), antimicrobial treatment, evaluation of food and water intake, and observation of clinical symptoms were all completed in the morning of each day. (B) Infection scores of symptoms. (C) *S. chromogenes* aggravated the clinical symptoms of birds infected with *Av. paragallinarum*. The difference was compared among the vancomycin treatment group and mono- or coinfection groups. (D) The food intake of each group was recorded every morning before renewal. (E) Body weight was recorded pre- and post-trial, and the weight obtained was calculated using subtraction. (F) Bacterial burden of the nasal cavity and infraorbital sinuses. (G) The bacterial community of the nasal cavity and infraorbital sinuses. (H) Serious tissue damage was observed in birds coinfecting with *S. chromogenes* and *Av. paragallinarum*. A large number of inflammatory cells infiltrated the epithelial tissue or were contained in the respiratory secretions (a). Epithelial cells were damaged and shed (b). Scale bar = 100  $\mu\text{m}$ . *P* values were determined by unpaired *t*-test. The mean of six biological replicates is shown, and error bars represent the standard deviation (SD) ( $n = 6$ ).

<https://doi.org/10.1371/journal.ppat.1009436.g005>

extensive infiltration of inflammatory cells and detachment of epithelial cells in the coinfecting group (Fig 5H), which are in agreement with previous reports that coinfection of *Av. paragallinarum* and other bacteria exacerbates the symptoms in birds [34, 35]. As expected, the removal of *S. chromogenes* by vancomycin significantly prevented the progression of disease caused by *Av. paragallinarum* and decreased the bacterial burden (Figs 5C–5H and S8). However, the burden of *Av. paragallinarum* in the tissue still reached approximately  $10^6$  CFUs/g in the absence of *S. chromogenes*. We deduced that the propagation of *Av. paragallinarum* may be directly promoted by the host because host cells might release  $\text{NAD}^+$  into the extracellular environment under conditions of inflammation or cellular stresses [14, 36]. Hence, our data indicate that resident *S. chromogenes* in the upper respiratory tract greatly promotes *Av. paragallinarum* infection in birds.

### ***S. chromogenes* and *Av. paragallinarum* promoted the synthesis and release of $\text{NAD}^+$**

To track the source of  $\text{NAD}^+$  derived from *S. chromogenes* and/or host cells, we employed a pulmonary epithelial cell line (A549) and macrophage cell line (MH-S) to explore the intrinsic relationship between hosts and bacteria. No propagation of *Av. paragallinarum* was observed in the absence of host cells (Figs 6A and S10A). Nevertheless, the number of *Av. paragallinarum* significantly increased and reached approximately 100-fold higher than the initial bacterial density in the presence of MH-S cells or A549 cells after incubation for 6 h. Comparably, the number of *Av. paragallinarum* increased approximately another 10-fold in the presence of *S. chromogenes* (Figs 6A and S10A and S10B). Subsequently, we quantified the  $\text{NAD}^+$  content in the supernatant of the cell cultures. In contrast to the threefold increase in extracellular  $\text{NAD}^+$  content with MH-S cells, the content of extracellular  $\text{NAD}^+$  increased approximately 10 times when cocultured with *S. chromogenes* (Fig 6B). Considering that *S. chromogenes* alone could not promote the growth of *Av. paragallinarum* (S10A Fig), the great accumulation of extracellular  $\text{NAD}^+$  was more likely to be released from host cells. Therefore, *S. chromogenes* should play a critical role in elevating the  $\text{NAD}^+$  level originating from host cells during coinfection.

To further investigate the release of  $\text{NAD}^+$  from host cells, we observed that *S. chromogenes* caused more severe membrane damage to all mammalian cells, particularly epithelial cells (Fig 6C), than *Av. paragallinarum*. Because  $\text{NAD}^+$  can be released from lysed cells into the extracellular environment [14], our results indicated that  $\text{NAD}^+$  may be passively released from host cells due to membrane damage. Interestingly, we found that the synthesis of  $\text{NAD}^+$  in host cells was activated by either *S. chromogenes* or *Av. paragallinarum* (Figs 6D, 6E and S10F and S13A). It seems that both bacteria tend to promote the production of NMN in host cells, a crucial intermediate for  $\text{NAD}^+$  biosynthesis [37], through the upregulation of two different pathways (Fig 7). Notably, the inhibition at the transcriptional level caused by *Av. paragallinarum* may not immediately reduce the amount of NMNAT1 (catalyzes the formation of  $\text{NAD}^+$  from

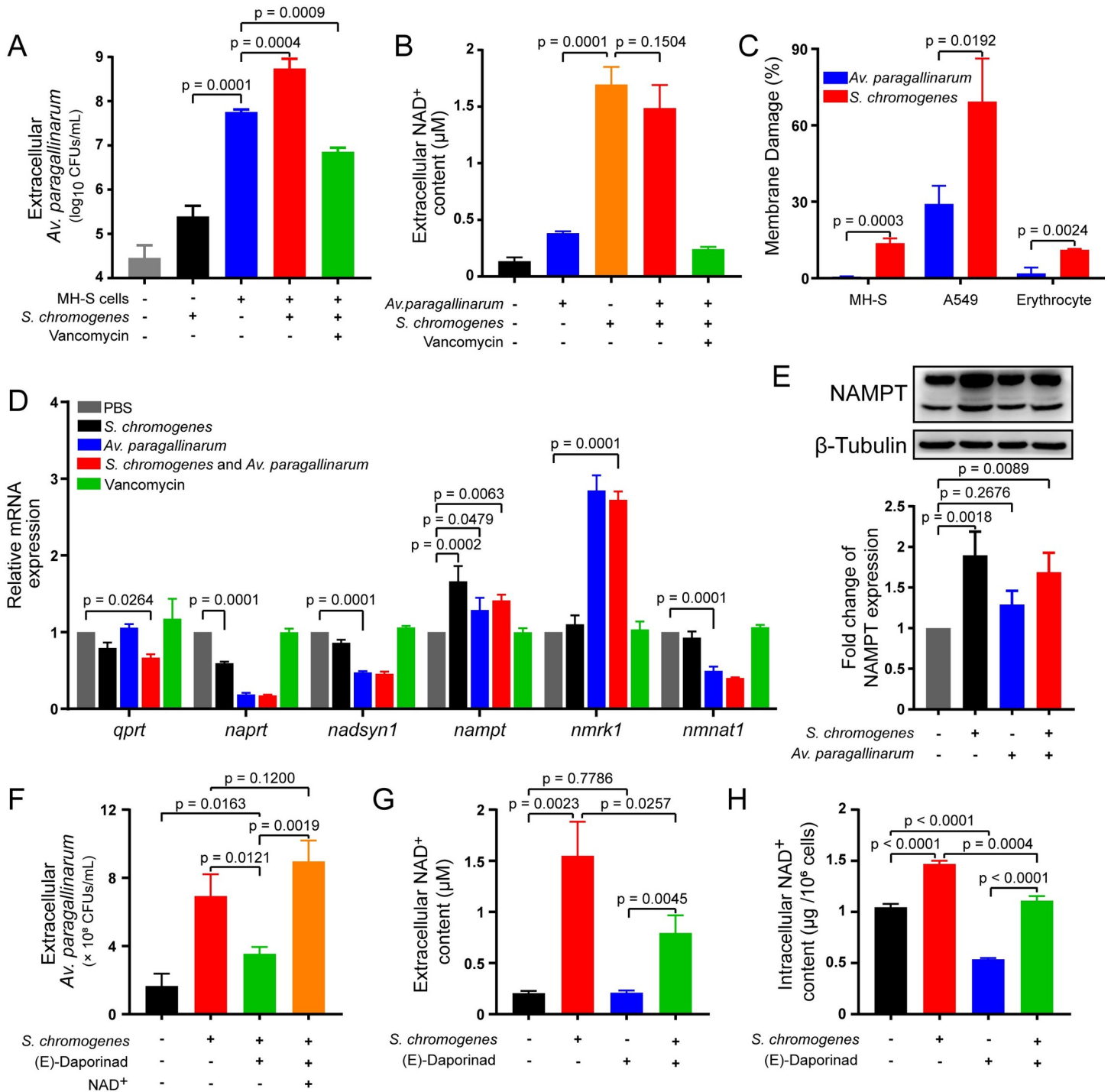


**Fig 6. *S. chromogenes* hijacks host cells to promote the growth of *Av. paragallinarum*.** (A) *S. chromogenes* increased the number of extracellular *Av. paragallinarum*. MH-S cells were infected with *S. chromogenes* SC10 and *Av. paragallinarum* X1-1S-1 (MOI = 1) and treated with 10 μg/mL vancomycin for 6 h. (B) *S. chromogenes* promoted NAD<sup>+</sup> release from the host cells. MH-S cells were treated the same as in (A). (C) *S. chromogenes* seriously damaged the membrane of mammalian cells. MH-S and A549 cells were infected with *S. chromogenes* SC10 (MOI = 1) for 6 h, and erythrocytes were coincubated with *S. chromogenes* (10<sup>6</sup> CFUs/mL) in PBS for 6 h. (D) The mRNA expression of NAD<sup>+</sup> synthetases. MH-S cells were infected with *S. chromogenes* SC10 and/or *Av. paragallinarum* X1-1S-1 (MOI = 1) or incubated with 10 μg/mL vancomycin for 6 h. (E) *S. chromogenes* promoted the expression of NAMPT. A549 cells were infected with *S. chromogenes* SC10 and/or *Av. paragallinarum* X1-1S-1 (MOI = 1) for 6 h. (F) The NAMPT inhibitor (E)-daporinad reduced the number of *Av. paragallinarum*. MH-S cells were infected with *S. chromogenes* SC10 and *Av. paragallinarum* X1-1S-1 (MOI = 1) and treated with 1 μM (E)-daporinad and/or 10 μg/mL exogenous NAD<sup>+</sup> for 6 h. (G, H) *S. chromogenes* increased the content of extracellular or intracellular NAD<sup>+</sup>. MH-S cells were infected with *S. chromogenes* (MOI = 1) and/or treated with 1 μM (E)-daporinad for 6 h. *P* values were determined by one-way ANOVA (A, B, D and E) and unpaired *t*-test (C, F, G and H). The mean of three biological replicates is shown, and error bars represent the standard deviation (SD) (n = 3).

<https://doi.org/10.1371/journal.ppat.1009436.g006>

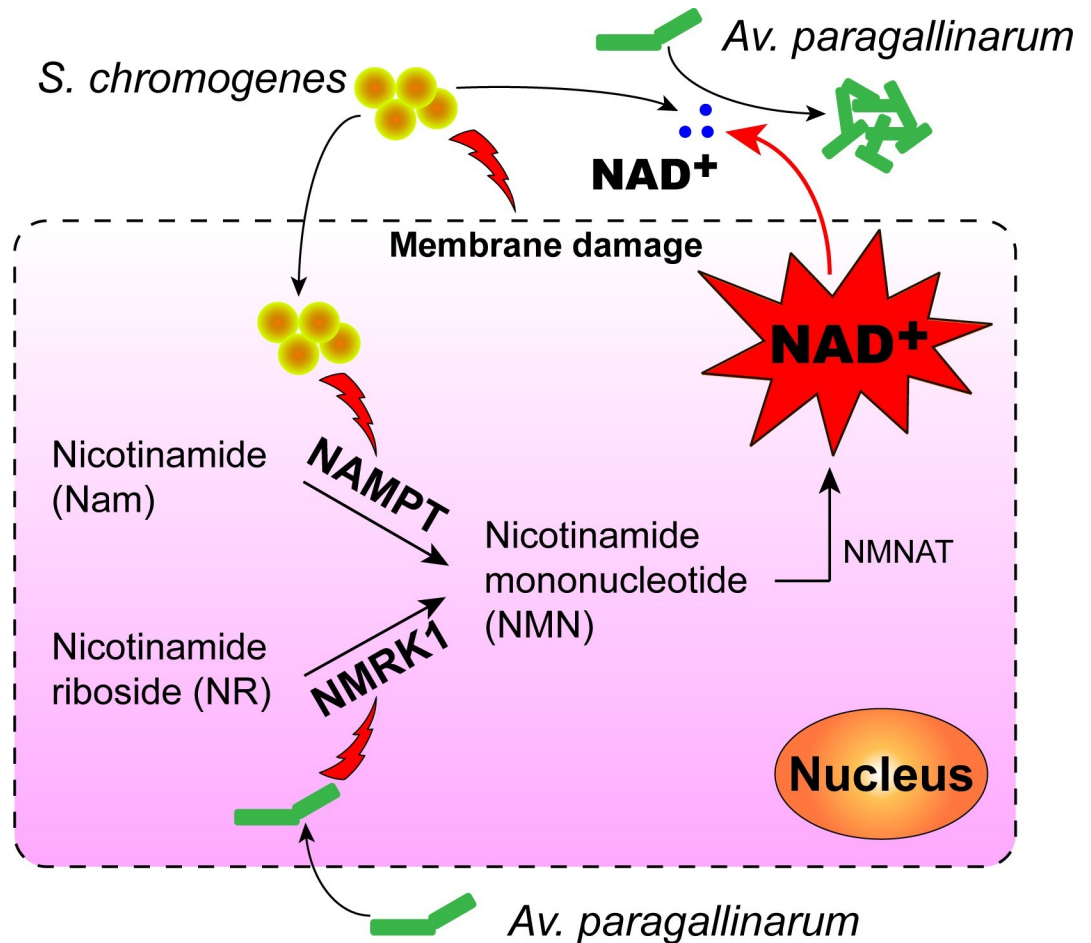


**Fig 7. Resident bacteria promote the replication of *Av. paragallinarum*.** Resident bacteria such as *S. chromogenes* enhance  $\text{NAD}^+$  biosynthesis and release by host cells in the respiratory tract. Consequently, the increased  $\text{NAD}^+$  level in the extracellular environment accelerates the replication of *Av. paragallinarum*.

<https://doi.org/10.1371/journal.ppat.1009436.g007>

NMN) and the downstream product  $\text{NAD}^+$  in the short term (S13B Fig). However, *Av. paragallinarum* may interrupt the homeostasis of intracellular  $\text{NAD}^+$  and induce the apoptosis of immune cells with persistent inhibition [38] to promote invasion.

Compared to other *Staphylococcus* isolates, such as *Staphylococcus warneri* and *S. aureus*, *S. chromogenes* showed a better growth-promoting effect on *Av. paragallinarum* by enhancing the expression of *namp1* (S12 Fig). Subsequently, we employed a specific inhibitor of NAMPT, (E)-daporinad [39], to test the role of NAMPT in the growth of *Av. paragallinarum*. (E)-Daporinad sharply reduced the number of extracellular *Av. paragallinarum*. Nevertheless, exogenous addition of  $\text{NAD}^+$  completely abolished this inhibitory effect (Figs 6F and S6B), as confirmed by the diminished extracellular and intracellular  $\text{NAD}^+$  contents (Fig 6G–6H). Therefore, these results highlight that  $\text{NAD}^+$  production in host cells is hijacked by *S. chromogenes* to promote the growth of *Av. paragallinarum*. Moreover, we observed the presence and survival of internalized *S. chromogenes* or *Av. paragallinarum* in epithelial cells and macrophages based on confocal microscopy analysis and gentamycin protection assays (S14A and S14B Fig), consistent with previous studies showing that *Haemophilus* spp. and other bacteria can also initiate intracellular survival [40–42]. Hence, we deduce that *S. chromogenes* not only promotes the growth of *Av. paragallinarum* under extracellular conditions but also increases

the intracellular burden of *Av. paragallinarum* (S14C and S14E Fig), through either directly facilitating the invasion of extracellular *Av. paragallinarum* or promoting the growth of internalized *Av. paragallinarum*. Altogether, our results indicate that *S. chromogenes* not only destabilizes the membrane of host cells but also induces the biosynthesis of NAD<sup>+</sup> to consequently promote *Av. paragallinarum* growth (Fig 7).

## Discussion

Our results highlight the contribution of resident bacteria to *Av. paragallinarum* infection in the respiratory tract and most likely the infection of other *Haemophilus* spp.. Resident bacteria such as *S. chromogenes* can not only directly supply NAD<sup>+</sup> to *Av. paragallinarum* but also reinforce the biosynthesis and release of NAD<sup>+</sup> in host cells. Hence, *Av. paragallinarum* succeeded in hijacking host cells to become its own NAD<sup>+</sup> sources (Fig 7). Our findings elucidate a better understanding of the infection caused by opportunistic pathogens in the respiratory tract and the development of new strategies to prevent and control such infections.

Commensal *Haemophilus* spp. are opportunistic pathogens that cause volatile infections [43]. Most *Haemophilus* need NAD<sup>+</sup> or NMN as an extra growth factor, whereas the level of such compounds usually cannot reach satisfactory concentrations for rapid bacterial replication in the respiratory tract of healthy individuals [10–12, 44]. Unexpectedly, we found that resident *S. chromogenes* along with other *Staphylococcus* isolates can produce additional NAD<sup>+</sup> (Figs 4A–4C and S7) to promote the survival of *Av. paragallinarum*. Consistent with our findings (S12 Fig), previous studies also suggest that the colonization of *H. influenzae* increases in hosts precolonized with either *S. aureus* or *Streptococcus pneumoniae*, which are resident bacteria in the upper respiratory tract [45, 46]. Mammalian cells have evolved three ways to produce NAD<sup>+</sup>. Coincidentally, both *S. chromogenes* and *Av. paragallinarum* activate the salvage pathway (Figs 6D and S10F), of which either the intermediate (NMN) or end-product (NAD<sup>+</sup>) can promote the growth of *Av. paragallinarum* [44]. This hijacking behavior suggests a novel synergistic infection in which opportunistic pathogens maximally plunder resources from host cells with the assistance of resident bacteria.

Interestingly, we found that *S. chromogenes* adapted better to high culturing temperatures at 42°C than at 37°C (Figs 3B and S7B). Previous reports indicate that tolerance to high temperatures is highly related to bacterial virulence for better investments in resource acquisition and other purposes [47, 48]. In contrast to those in bovine-originating *S. chromogenes* [29, 49], the diversity of virulence genes in bird-derived isolates is much lower (S5 Fig). The compromise of the survival of *S. chromogenes* may attenuate its pathogenicity to hosts, which is consistent with our observation that clinical symptoms were barely recognized after birds were infected solely with *S. chromogenes* (S9 Fig). Notably, temperature adaptability may explain its irreplaceable role in infections of the avian respiratory tract due to intrinsically high body temperatures ranging from 40 to 43°C.

Although we have demonstrated that resident bacteria make great contributions to infections, how *Av. paragallinarum* evades innate immune killing and the restriction of local microbial communities to acquire a replication niche remain unclear. Moreover, vaccination is the most important strategy against IC, and the combined immunization of *S. chromogenes* and *Av. paragallinarum* to produce better outcomes needs further evaluation.

## Materials and methods

### Epidemiological investigation

We undertook a study to investigate the prevalence of infectious coryza (IC) in 2019. Natural and anthropogenic data from 14 provinces and municipalities in China were collected by

questionnaires shared on the internet. Multiple anthropogenic and natural factors were included. Statistical analyses were based on previously described methods [50]. Variables with  $P < 0.05$  were kept in the final model.

### Bacterial isolation and culture

Twenty birds with typical facial edema and discharges in the nasal cavity and infraorbital sinuses were sacrificed for bacterial isolation. The heads of birds were covered with 75% ethyl alcohol to avoid contamination. Samples were collected from the nasal cavity and infraorbital sinuses when beaks were cut and jowls were slit after the volatilization of ethyl alcohol. The discovery method was culture-based isolation. In detail, the initial inoculations were performed on blood agar plates, and tryptic soy agar plates (TSA, Beijing Land Bridge Technology Co., China) supplemented with 5% (v/v) fetal bovine serum (FBS, Gibco, Thermo Fisher Scientific, US) and 0.001% (w/v) nicotinamide adenine dinucleotide (NAD<sup>+</sup>, Sigma-Aldrich, Merck Millipore, US) were used at the same time. Samples were then incubated in a 5% CO<sub>2</sub> incubator at 37°C for 48 h. The suspected colonies of *Av. paragallinarum* were then cultured in tryptic soy broth (TSB, Beijing Land Bridge Technology Co., China) supplemented with 5% (v/v) FBS and 0.0025% (w/v) NAD<sup>+</sup>. Other colonies were cultured in TSB for further identification.

### Antibacterial tests

The minimal inhibitory concentrations (MICs) of different antibiotics for bacteria were determined using the broth microdilution method according to the Clinical and Laboratory Standards Institute criteria described in documents VET08 and M100-S28 [51, 52]. Briefly, antibiotics were diluted twofold in Mueller–Hinton broth (MHB, Beijing Land Bridge Technology Co., China) and mixed with an equal volume of bacterial suspensions in MHB containing approximately  $1.5 \times 10^6$  colony-forming units (CFUs)/mL in a clear, UV-sterilized, 96-well microtiter plate (Corning Incorporated Co., US). After *S. chromogenes* was cultured for 18 h at 37°C, the MICs were defined as the lowest concentrations of antibiotics with no visible growth of bacteria. For *Av. paragallinarum* isolates, the only modification was the broth used: cation-adjusted Mueller-Hinton broth (CAMHB, Shanghai GuanDao Biotech Co., China) plus 0.0025% (w/v) NAD<sup>+</sup> and 1% (v/v) sterile-filtered heat-inactivated chicken serum (Solarbio Life Science Co., China). Additionally, the standard quality control strains for MIC tests were *S. aureus* American Type Culture Collection (ATCC) 29213 and *E. coli* ATCC 25922.

### Bacterial identification and serotyping of *Av. paragallinarum* isolates

The identification of bacterial species was conducted by matrix-assisted laser desorption/ionization time-of-flight (MALDI-TOF) mass spectrometry analysis and 16S rRNA gene sequencing. DNA was extracted from all isolates using a TIANamp Bacteria DNA Kit (Tiangen Biotech Co., Beijing, China) according to the manufacturer's instructions. *Av. paragallinarum* isolates were serotyped using multiplex polymerase chain reaction (mPCR) to identify serogroups (A, B, and C), as previously described [25]. The isolation rates and colocalization rates were calculated by the following formulae.

Isolation rate: the number of bacteria of a specific genus/total number of samples.

Colocalization rate: the number of birds infected with a specific genus of bacteria and *Av. paragallinarum*/the number of birds infected with *Av. paragallinarum*.

## Satellitism

The workflow of these experiments referred to a previously described method, with some modifications [23]. The *Av. paragallinarum* isolates X1-1S-1 and 12-4N-1 and *Haemophilus parasuis* 17CQ1B34-2 [32] were selected for the tests. Briefly, 100  $\mu$ L of phosphate-buffered saline (PBS, pH = 7.4) suspension of *Av. paragallinarum* ( $10^6$  CFUs/mL) prepared from 24-hour growth on a TSA plate supplemented with FBS and NAD<sup>+</sup> was plated on a sheep blood agar plate. The overnight growth of bacteria of other genera was adjusted to McFarland 0.5 turbidity in 0.9% NaCl solution, and 2  $\mu$ L of suspension was subsequently inoculated onto the blood agar plates, which were covered with *Av. paragallinarum* or *H. parasuis*. When the droplets were dry, the plates were incubated in a 5% CO<sub>2</sub> incubator at 37°C. The radii of satellitism were measured after incubation for 48 h. *S. aureus* ATCC 29213 and methicillin-resistant T144 [53] were set as reference strains.

## Growth curves and bacterial time-killing curves

The workflow of these experiments referred to a previously described method, with some modifications [54]. Briefly, overnight cultures of the *S. chromogenes* isolate SC10, *Staphylococcus agnetis* isolate 12-4S-3, *S. aureus* isolate 12-1N-1, *Staphylococcus haemolyticus* isolate X2-2N-1, *Staphylococcus warneri* isolate X1-2S-2, *Staphylococcus pseudintermedius* isolate 29HD2S-5 and *Staphylococcus sciuri* isolate Z1S-3 were adjusted to McFarland 0.5 turbidity and diluted 1:100 in TSB medium. The overnight culture of the *Av. paragallinarum* isolate X1-1S-1 was adjusted to McFarland 0.5 turbidity and diluted 1:100 in TSB medium supplemented with 5% (v/v) FBS and 0.0025% (w/v) NAD<sup>+</sup>. Alternatively, 0.02% Triton, 16  $\mu$ g/mL clindamycin, 64  $\mu$ g/mL vancomycin, or 2  $\mu$ M (E)-daporinad (MedChemExpress Co., US) was added to a 96-well microplate and mixed with an equal volume of bacterial culture with the plate lid covering. The overnight culture of the *S. chromogenes* isolate SC10 was adjusted to McFarland 0.5 turbidity and diluted 1:100 in TSB medium supplemented with 5% (v/v) FBS. (E)-Daporinad (2  $\mu$ M) was added to a 96-well microplate and mixed with an equal volume of bacterial culture with the plate lid covering. The growth curves were recorded afterward at a wavelength of 600 nm, with an interval of 1 h at 37°C or 42°C, using an Infinite M200 Microplate reader (Tecan Co., Switzerland) in the long-term model.

The workflow of bacterial time-killing curve experiments was performed according to a previously described method, with some modifications [53]. The overnight cultures of the *S. chromogenes* isolate SC10 and *Av. paragallinarum* isolate X1-1S-1 were adjusted to McFarland 0.5 turbidity and diluted 1:100 in TSB medium supplemented with 5% (v/v) sheep blood. In addition, vancomycin and clindamycin (Aladdin Biochemical Technology Co., Shanghai, China) were applied at 32  $\mu$ g/mL and 8  $\mu$ g/mL, respectively. All media were cultured in 12 mL sterile culture tubes (Haimen United Laboratory Equipment Development Co., Jiangsu, China), the caps of which were equipped with filters so the gas could be normally exchanged. The suspension of all experiments was serially diluted tenfold and plated on solid medium, with incubation at 37°C for 24 h. TSA plates were applied for the detection of *S. chromogenes*, while TSA plates supplemented with 5% (v/v) FBS, 0.001% (w/v) NAD<sup>+</sup> and 10  $\mu$ g/mL vancomycin were used for the examination of *Av. paragallinarum*.

## Coculture of *S. chromogenes* and *Av. paragallinarum* in vitro

Overnight cultures of the *S. chromogenes* isolate SC10, *Av. paragallinarum* isolate X1-1S-1, *Enterococcus faecalis* isolate 29HD2S-2 (from this research), *S. sciuri* isolate Z1S-3, and *H. parasuis* isolate 17CQ1B34-2 were first adjusted to McFarland 0.5 turbidity in TSB. Blood was heated at 85°C for 10 min. Erythrocytes and serum were separated by centrifugation of fresh

blood at  $500 \times g$  for 10 min, and erythrocytes were resuspended in isovolumetric 0.9% NaCl solution. Bacterial suspensions were diluted 1:100 in TSB medium supplemented with 5% (v/v) heated blood, fresh blood, fresh blood with 0.01% (v/v) Triton, resuspended erythrocytes or isolated serum separately or together. The numbers of *Av. paragallinarum* in the medium were detected by plating serial dilutions on TSA supplemented with 5% (v/v) FBS and 0.0025% (w/v)  $\text{NAD}^+$  after bacterial culture for 6 h at 37°C.

### Whole genome sequencing analysis

DNA extraction, library construction, sequencing, assembly, and construction of SNP-based phylogenetic trees were completed according to a previous report [55]. Antibiotic resistance genes were identified using BLAST in a custom database, and virulence genes of *Av. paragallinarum* and *S. chromogenes* isolates were identified using BLAST by a custom database retrieved from VFDB (<http://www.mgc.ac.cn/cgi-bin/VFs/compvfs.cgi?Genus=Haemophilus>, <http://www.mgc.ac.cn/cgi-bin/VFs/compvfs.cgi?Genus=Staphylococcus>). The whole-genome sequences of *Av. paragallinarum* and *S. chromogenes* isolates investigated in this study have been deposited at GenBank under accession numbers PRJNA648655 and PRJNA648661.

### Ethics statement

All animal protocols were approved by the Genentech Institutional Animal Care and Use Committee at China Agricultural University (SYXK, 2018–0038). The experimental procedures involving birds gained approval (AW40300202-2).

### Birds and animal regression test

Male specific pathogen-free (SPF) white leghorn chickens aged five weeks were obtained from Beijing Boehringer Ingelheim Vital Biotechnology Co., Ltd. Birds were randomly divided into four groups with six birds in each group and adapted to standardized environmental conditions under negative pressure for one week before infection. Overnight cultures of the *S. chromogenes* isolate SC10 and *Av. paragallinarum* isolate X1-1S-1 were resuspended in 200  $\mu\text{L}$  of 0.9% saline solution at  $1 \times 10^9$  CFUs per bird, and vancomycin was prepared at a concentration of 32  $\mu\text{g}/\text{mL}$ . Vancomycin treatment and bacterial infection were both applied by injection in the infraorbital sinuses, with a volume of 200  $\mu\text{L}$ . On the last day of the experiments, all birds were sacrificed. The tissues of the nasal cavity and infraorbital sinuses were removed and homogenized in sterile PBS for the determination of bacterial load and metagenome analysis, or tissue was removed and fixed in 4% paraformaldehyde for hematoxylin and eosin (H & E) staining.

### Clinical scoring

Birds were examined daily, and clinical signs were scored and recorded every morning throughout the whole experiment according to a previously reported scale [35]: 0, no clinical signs; 1, mild nasal discharge or swelling of the infraorbital sinuses; 2, nasal discharge along with swelling of the infraorbital sinuses; and 3, severe swelling of the infraorbital sinuses with or without conjunctivitis. The body weights of birds were recorded pre- and post-trial. The food and water intakes of each group of birds were measured and recorded every morning before renewal.

## Bacterial community characterization

Bacterial community characterization was performed according to previously described research [56]. Briefly, tissue samples of the nasal cavity and infraorbital sinuses were collected and homogenized in sterile PBS. The V3-V4 regions of microbial 16S rDNA genes were amplified and purified, and sequencing was performed at an institute authorized to sequence environmental genomics (Sinobiocore Inc., Beijing, China). Raw fastq files were demultiplexed using barcode sequences (<https://github.com/jameslz/div-utils/blob/master/div-utils> version: 0.0.1-r1-dirty). Quality filtering was performed using Trimmomatic [57], and paired reads were merged using the USEARCH fastq\_mergepairs command [58]. Operational taxonomic units (OTUs) were clustered with a 97% similarity cutoff using USEARCH UPARSE [59], and the chimeric sequences were removed in the UPARSE pipeline. The raw sequence reads have been deposited in the NCBI Sequence Read Archive under accession number PRJNA646660.

## Cell lines and cell culture

Human lung carcinoma epithelial cells (A549) and mouse lung macrophages (MH-S) were cultured in Dulbecco's modified Eagle's medium (DMEM, Thermo Fisher Scientific, US) or Roswell Park Memorial Institute (RPMI)-1640 medium (Thermo Fisher Scientific, US) supplemented with 10% FBS and 1% (w/v) penicillin-streptomycin (Solarbio Life Science Co., Shanghai, China). All cells were cultured at 37°C in a 5% CO<sub>2</sub> atmosphere. All cell lines were obtained from the ATCC.

## Cell infection

A549 and MH-S cells were seeded in antibiotic-free medium at a concentration of  $0.5 \times 10^6$  cells per well in 24-well plates (Corning Incorporated Co., US). Cells were infected with the *S. chromogenes* isolate SC10, *S. aureus* isolate 12-1N-1, *S. warneri* isolate X1-2S-2, *Av. paragallinarum* isolate X1-1S-1, or *E. faecalis* isolate 29HD2S-2 (from this research) at a multiplicity of infection (MOI) of 1 and treated with 32 µg/mL vancomycin for 6 h. The numbers of *Av. paragallinarum* in the supernatant of cell cultures were subsequently detected by plating serial dilutions on TSA supplemented with 5% (v/v) FBS and 0.0025% (w/v) NAD<sup>+</sup>.

MH-S and A549 cells were seeded at  $1 \times 10^6$  cells per well in 12-well culture plates (Corning Incorporated Co., US) to form monolayers. Overnight cultures of the *S. chromogenes* isolate SC10 and *Av. paragallinarum* isolate X1-1S-1 were resuspended in PBS. Finally, bacterial resuspensions were diluted in DMEM or RPMI-1640 medium supplemented with 1% FBS and cocultured with A549 and MH-S cells at an MOI of 1 for 6 h. At the end of the trials, 100 µg/mL gentamycin was applied to remove the extracellular bacteria, and the counting of intracellular bacteria was followed by host cell lysis and serial dilution.

## Detection of membrane damage and cytotoxicity tests

Erythrocytes were harvested by centrifugation of fresh sheep blood at  $500 \times g$  for 10 min and subsequently resuspended in isovolumetric 0.9% NaCl solution. Overnight cultures of the *S. chromogenes* isolate SC10 or *Av. paragallinarum* isolate X1-1S-1 were standardized to match a 0.5 McFarland turbidity followed by a 1:100 dilution in PBS supplemented with a 10% (v/v) suspension of erythrocytes for 6 h at 37°C. After that, the fluids were first centrifuged at  $500 \times g$  for 10 min, and 200 µL of supernatants were centrifuged for another 2 min at  $10000 \times g$ . The membrane damage of erythrocytes was evaluated by detecting the released lactate dehydrogenase (LDH) in the supernatant.

A549 and MH-S cells were seeded in antibiotic-free medium at a concentration of  $0.5 \times 10^6$  cells per well in 24-well plates. Host cells were infected with *S. chromogenes* or *Av. paragallinarum* at an MOI of 1 or incubated with 0.01% Triton (Beyotime Biotechnology Co., Shanghai, China) as a positive control for 6 h. Supernatants of cell cultures were then acquired by centrifugation at  $1000 \times g$  for 5 min at 4°C. The levels of LDH in the supernatants were detected by an LDH cytotoxicity assay detection kit (Beyotime Biotechnology Co., Shanghai, China) following the manufacturer's instructions.

Cytotoxicity examinations on mammalian cells were performed on A549 and MH-S cells using an LDH cytotoxicity assay detection kit following the manufacturer's instructions. (E)-Daporinad (2–0.015625  $\mu\text{M}$ ) and  $1 \times 10^4$  cells were simultaneously added to 96-well plates. Cells were cultured in DMEM or RPMI-1640 medium supplemented with 1% heat-inactivated FBS and 1% (w/v) penicillin-streptomycin at 37°C in a 5% CO<sub>2</sub> atmosphere for 12 h, followed by LDH tests.

### Detection of NAD<sup>+</sup>

Overnight cultures of different *Staphylococcus* isolates were standardized to match a 0.5 McFarland turbidity followed by a 1:100 dilution in TSB medium supplemented with 5% (v/v) FBS. The *S. chromogenes* isolate SC10 was cultured at 37°C for different times or at 42°C for 4 h. The *S. chromogenes* isolates SC1, SC2, SC5, SC14, and SC24 and other *Staphylococcus* isolates were cultured at 37°C for 4 h. Two hundred microliters of bacterial culture supernatant was obtained by centrifugation at  $10000 \times g$  for 2 min at 4°C.

MH-S and A549 cells were seeded in antibiotic-free medium at a concentration of  $0.5 \times 10^6$  cells per well in 24-well plates. Cells were then infected with the *S. chromogenes* isolate SC10 or *Av. paragallinarum* isolate X1-1S-1 at an MOI of 1 at 37°C for 6 h. In addition, infected MH-S cells were incubated with 32  $\mu\text{g}/\text{mL}$  vancomycin or 1  $\mu\text{M}$  (E)-daporinad at 37°C for 6 h. A549 cells were incubated with 0.01% Triton or 1  $\mu\text{g}/\text{mL}$  LPS (Sigma-Aldrich, Merck Millipore, US) at 37°C for 6 h. The supernatants of cell cultures were acquired by centrifugation at  $1000 \times g$  for 5 min at 4°C. The extracellular or intracellular NAD<sup>+</sup> levels were measured by an NAD<sup>+</sup>/NADH Assay Kit with WST-8 (Beyotime Biotechnology Co., Shanghai, China) following the manufacturer's instructions.

### RT-qPCR analysis

RT-qPCR analyses were performed according to previously described research [60]. Briefly, MH-S and A549 cells were seeded in antibiotic-free medium at a concentration of  $2 \times 10^6$  cells per well in 6-well plates (Corning Incorporated Co., US). After that, the cells were infected with *S. chromogenes* SC10, SC1, SC2, SC5, SC14, or SC24; *Av. paragallinarum* X1-1S-1; *S. aureus* 12-1N-1; or *S. warneri* X1-2S-2 at an MOI of 1 or treated with 32  $\mu\text{g}/\text{mL}$  vancomycin at 37°C for 6 h. Total RNA was extracted using a HiPure Total RNA Plus Mini Kit (Magen Biotechnology Co., Guangzhou, China), and 1  $\mu\text{g}$  of extracted RNA was reverse transcribed with a PrimeScript RT Reagent Kit (TaKaRa Bio incorporated, Japan) following the manufacturer's protocol. The messenger RNA levels of *qprt*, *naprt*, *nadsyn1*, *nampt*, *nmrk1* and *nmmat1* relative to those of the control genes *gapdh* or *actb* in MH-S or A549 cells were determined by real-time PCR tests with PowerUp SYBR Green Master Mix (Applied Biosystems, Thermo Fisher Scientific, US). RT-PCR tests were performed using the ABI Quantstudio 7 detection system (Applied Biosystems, Thermo Fisher Scientific, US). The fold changes in gene expression were determined using the  $2^{-\Delta\Delta C_t}$  method. The primer sequences are listed in S6 Table.

## Western blotting

Western blotting was utilized to analyze the expression of NAMPT and NMRK1. A549 cells were seeded in antibiotic-free medium at a concentration of  $2 \times 10^6$  cells per well in 6-well plates. Cells were then infected with the *S. chromogenes* isolate SC10 and/or *Av. paragallinarum* isolate X1-1S-1 at an MOI of 1 at 37°C for 6 h. The primary antibodies included rabbit anti-NAMPT (Invitrogen, Thermo Fisher Scientific, US), rabbit anti-NRK1 (Abcam Co., UK) and rabbit anti- $\beta$ -tubulin antibodies (Cell Signaling Technology, US). The secondary antibody was a goat anti-rabbit antibody (Beyotime Biotechnology Co., Shanghai, China). Gray values of protein bands were quantified by ImageJ software.

## Confocal laser scanning microscopy analysis

A549 cells were seeded in antibiotic-free medium at a concentration of  $0.5 \times 10^6$  cells per well in 24-well glass-bottom plates (NEST Life and Science Technology Co., Wuxi, China). Host cells were infected with pHrodoRed-labeled (Invitrogen, Thermo Fisher Scientific, US) *S. chromogenes* or *Av. paragallinarum* at an MOI of 20 for 1 h, followed by fixation in 4% paraformaldehyde. F-actin was stained with ActinGreen 488 ReadyProbes, and the nuclei were counterstained with DAPI (Beyotime Biotechnology Co., Shanghai, China).

For static images, fixed and stained cellular samples were captured by a Leica SP8 confocal microscope. To analyze the location of internalized bacteria, the Z-axis sections were cut every 0.3  $\mu$ m. Images were analyzed and merged by LAS AF Lite software (Leica Biosystems, Germany).

## Statistical analysis

Statistical analysis was performed using GraphPad Prism 7.0 (GraphPad Software, Inc.). *p*-values were calculated using an unpaired *t*-test with Bonferroni correction between two groups or a nonparametric one-way ANOVA among multiple groups. All data are expressed as the mean  $\pm$  SD. All experiments were performed on no less than three biological replicates.

## Supporting information

**S1 Data.** Excel spreadsheet containing, in separate sheets, the underlying numerical data and statistical analysis for Figure panels 1D, 2B, 2C, 3B, 4A, 4B, 4C, 5C, 5D, 5E, 5F, 5G, 6A, 6B, 6C, 6D, 6E, 6F, 6G and 6H.

(XLSX)

**S2 Data.** Excel spreadsheet containing, in separate sheets, the underlying numerical data and statistical analysis for panels S3, S4, S6A, S6B, S7A, S7B, S7C, S7D, S8, S9, S10A, S10B, S10C, S10D, S10E, S10F, S11, S12, S13A, S13B, S14B, S14C, S14D and S14E Figs.

(XLSX)

**S1 Table.** Descriptive and univariable analysis of the variables of interest. \*, Significant variable in univariable analysis ( $P \leq 0.05$ ). NA, not applicable.

(XLSX)

**S2 Table.** Descriptive and univariable analysis of factors associated with recurrent IC outbreaks. \*, Significant variable in univariable analysis ( $P \leq 0.05$ ). NA, not applicable.

(XLSX)

**S3 Table.** Bacteria isolated from the respiratory tract of birds (excluding *Av. paragallinarum*). a, Colocalization rate: the number of birds infected with a specific genus of bacteria

and *Av. paragallinarum*/the number of birds infected with *Av. paragallinarum*.  
(XLSX)

**S4 Table. MICs of all tested antibiotics to *Av. paragallinarum*.** FLO, florfenicol; CLI, clindamycin; ERY, erythromycin; CEF, cefoxitin; TET, tetracycline; OXA, oxacillin; ENR, enrofloxacin; TRI/SUL, trimethoprim/ sulfamethoxazole; GEN, gentamycin; PEN, penicillin; AMP, ampicillin; TIL, tilmicosin; AMO/CLA, amoxicillin/ clavulanic acid; MER, meropenem; POL, polymyxin E. a, Data represent the concentration of trimethoprim. b, Data represent the concentration of amoxicillin. c, The number of isolates with MIC values equal to or higher than the concentrations of tested ranges. d, The number of isolates with MIC values equal to or lower than the concentrations of tested ranges.  
(XLSX)

**S5 Table. MICs of all tested antibiotics to *S. chromogenes*.** MICs of antibiotics in µg/mL; PEN, penicillin; OXA, oxacillin; AMO/CLA, amoxicillin/clavulanic acid (2: 1); CEF, cefoxitin; ERY, erythromycin; TET, tetracycline; GEN, gentamycin; CLI, clindamycin; TIA, tiamulin; ENR, enrofloxacin; LIN, linezolid; RIF, rifampicin; VAN, vancomycin; TIL, tilmicosin; FLO, florfenicol; TRI/SUL, trimethoprim/sulfamethoxazole (1: 19).  
(XLSX)

**S6 Table. RT-PCR primer sets in this study.** \*, Primers were obtained from PrimerBank (<https://pga.mgh.harvard.edu/primerbank/index.html>). References corresponding to primers: mice-*naprt* [61]; mice-*nampt* [62]; mice-*nmrk1* [63]; mice-*nmnat1*, mice-*gapdh* [64]; Human-*naprt*, Human-*nadsyn1*, Human-*nampt*, Human-*nmrk1* [60]; Human-*nmnat1* [65]; Human-*actb* [66].  
(XLSX)

**S1 Fig. Mapped IC cases in China.** Prevalence of IC in China: data from 103 poultry farms were collected by questionnaires shared on the internet. Map layers were obtained from Wikimedia Commons (<https://commons.wikimedia.org/wiki/File:China-outline.svg>).  
(TIF)

**S2 Fig. Genetic Characteristics of *Av. paragallinarum* and *S. chromogenes* isolates.** Core-genome SNP-based phylogenetic trees of *Av. paragallinarum* (A) and *S. chromogenes* (B). Bacteria of the two genera were divided into two genotypes (labeled with blue and green), respectively. \*, reference strain. Distant genetic relationships are highlighted by red-colored connections and values.  
(TIF)

**S3 Fig. The radii of satellitism.** (A, B) *Av. paragallinarum* and bacteria of other species were cocultured on blood agar plates for 48 h, and the radii of satellitism generated by the *Av. paragallinarum* isolates 12-4N-1 (A) and X1-1S-1 (B) were measured. *P* values were determined by one-way ANOVA. The mean of radii is shown, and error bars represent the standard deviation (SD).  
(TIF)

**S4 Fig. Antimicrobial phenotype and genotype of *Av. paragallinarum* and *S. chromogenes* isolates.** The MICs of different antimicrobial agents to *Av. paragallinarum* (A) and *S. chromogenes* (B) were determined by the broth microdilution method. *Av. paragallinarum* isolates were serotyped through a mPCR assay to identify the serogroups. Antibiotic resistance genes in *Av. paragallinarum* and *S. chromogenes* isolates were identified using BLAST with a custom database. NA, nontypable. \*, sequence identities of *tet(38)* in all isolates and *ant(6)-Ia* in the

isolates *S. chromogenes* SC24, SC25, SC23, SC17, SC14 and SC22 were between 70% and 80%. Note: Multiple antibiotic-resistant phenotypes of most *Av. paragallinarum* were irrelevant to their genotypes. Similar to that of other Gram-negative bacteria, the outer membrane of *Av. paragallinarum* acts as a permeability barrier and prevents antibiotics from reaching their targets. In addition, resistance-mediating mutations are commonly seen in *Pasteurellaceae* of veterinary origin [67, 68]. Therefore, we hypothesized that *Av. paragallinarum* isolates may also evolve some gene mutations under the pressure of drugs and present different antimicrobial-resistant phenotypes.

(TIF)

**S5 Fig. Virulence genes carried by *S. chromogenes* and *Av. paragallinarum*.** All *S. chromogenes* (n = 25) (A) and *Av. paragallinarum* isolates (n = 18) (B) were divided into two clusters with different colors (blue and green), respectively. Virulence genes were analyzed based on whole-genome sequencing and custom databases retrieved from VFDB (<http://www.mgc.ac.cn/cgi-bin/VFs/compvfs.cgi?Genus=Haemophilus>, [http://www.mgc.ac.cn/cgi-bin/VFs/compvfs.cgi?Genus = Staphylococcus](http://www.mgc.ac.cn/cgi-bin/VFs/compvfs.cgi?Genus=Staphylococcus)).

(TIF)

**S6 Fig. Growth curves of *Av. paragallinarum* and *S. chromogenes*.** (A) Growth curves of *Av. paragallinarum* X1-1S-1 in the presence of 0.01% Triton, clindamycin (8 µg/mL), and vancomycin (32 µg/mL) for 24 h. The culture medium was TSB supplemented with 5% (v/v) serum and 0.0025% (w/v) NAD<sup>+</sup>. (B) Growth curves of *Av. paragallinarum* X1-1S-1 and *S. chromogenes* SC10 in the presence of 1 µM (E)-daporinad for 24 h. The culture medium for *Av. paragallinarum* was TSB supplemented with 5% (v/v) serum and 0.0025% (w/v) NAD<sup>+</sup>, and the culture medium for *S. chromogenes* was TSB supplemented with 5% (v/v) serum. The mean of six biological replicates is shown.

(TIF)

**S7 Fig. Different *Staphylococcus* species promote the survival of *Av. paragallinarum*.** (A, B) Bacteria were cultured in TSB supplemented with 5% serum. Bacteria were cultured at 37°C (A) or 42°C (B). The mean of six biological replicates is shown. (C) High culture temperature promoted NAD<sup>+</sup> production in *S. chromogenes*. *S. chromogenes* and *S. sciuri* were cultured in TSB supplemented with 5% serum for 4 h at 37°C or 42°C. *P* values were determined by one-way ANOVA. (D) *S. chromogenes* and *S. sciuri* showed no difference in promoting the survival of *Av. paragallinarum*. *P* values were determined by unpaired *t*-test. The mean of three biological replicates is shown, and error bars represent the standard deviation (SD) (n = 3).

(TIF)

**S8 Fig. Water intake is greatly reduced when birds are coinfecting with *S. chromogenes* and *Av. paragallinarum*.** The water intake of each group was measured and recorded every morning before the renewal of drinking water.

(TIF)

**S9 Fig. Mono-infection of *S. chromogenes* hardly triggers clinical symptoms.** The mean of six biological replicates is shown, and error bars represent the standard deviation (SD) (n = 6).

(TIF)

**S10 Fig. *S. chromogenes* and *Av. paragallinarum* induce NAD<sup>+</sup> production in host cells.** (A) Replication rates of extracellular *Av. paragallinarum* compared to that of the initial inoculum. MH-S cells were infected with *Av. paragallinarum* X1-1S-1 (MOI = 1) alone or accompanied by *S. chromogenes* SC10 (MOI = 1) for 6 h. (B) *S. chromogenes* increased the number of

extracellular *Av. paragallinarum*. MH-S or A549 cells were infected with *Av. paragallinarum* X1-1S-1 and/or *S. chromogenes* SC10 (MOI = 1) or incubated with 10  $\mu\text{g}/\text{mL}$  vancomycin for 6 h. (C) *S. chromogenes* increased the abundance of extracellular  $\text{NAD}^+$ . A549 cells were infected with *S. chromogenes* SC10 (MOI = 1) or incubated with 0.01% Triton or 1  $\mu\text{g}/\text{mL}$  LPS for 6 h. (D) *S. chromogenes* impaired the integrity of A549 cells. A549 cells were infected with *S. chromogenes* SC10 (MOI = 1) or incubated with 0.01% Triton for 6 h. (E) LPS treatment produced no difference in the extracellular  $\text{NAD}^+$  content. MH-S cells were incubated with 1  $\mu\text{g}/\text{mL}$  LPS for 6 h. (F) *S. chromogenes* and *Av. paragallinarum* increased the mRNA expression of *nampt* and *nmrk1*. A549 cells were infected with *S. chromogenes* SC10 and/or *Av. paragallinarum* X1-1S-1 (MOI = 1) or incubated with 10  $\mu\text{g}/\text{mL}$  vancomycin for 6 h. *P* values were determined by unpaired *t*-test for (A, B, D and E) and one-way ANOVA for (C and F). The mean of three biological replicates is shown, and error bars represent the standard deviation (SD) ( $n = 3$ ). (TIF)

**S11 Fig. (E)-Daporinad exhibits no cytotoxicity to respiratory cells.** The cytotoxicity of (E)-daporinad to A549 and MH-S cells was determined through an LDH release assay. The mean of three biological replicates is shown, and error bars represent the standard deviation (SD) ( $n = 3$ ). (TIF)

**S12 Fig. The extracellular growth of *Av. paragallinarum* is promoted by different *Staphylococcus* species.** A549 cells were monoinfected with *Staphylococcus* spp. (MOI = 1) for 6 h to examine the mRNA expression of  $\text{NAD}^+$  synthetases, or A549 cells were coinfecting with *Av. paragallinarum* X1-1S-1 and *Staphylococcus* spp. (MOI = 1) for 6 h to measure the number of extracellular *Av. paragallinarum*. *P* values were determined by one-way ANOVA. The mean of three biological replicates is shown, and error bars represent the standard deviation (SD) ( $n = 3$ ). (TIF)

**S13 Fig. *Av. paragallinarum* enhances  $\text{NAD}^+$  biosynthesis in host cells.** (A) *Av. paragallinarum* promoted the expression of NMRK1. A549 cells were infected with *S. chromogenes* SC10 and/or *Av. paragallinarum* X1-1S-1 (MOI = 1) for 6 h. *P* values were determined by one-way ANOVA. (B) *Av. paragallinarum* increased the intracellular  $\text{NAD}^+$  content. MH-S cells were infected with *Av. paragallinarum* X1-1S-1 (MOI = 1) for different times. *P* values were determined by unpaired *t*-test. The mean of three biological replicates is shown, and error bars represent the standard deviation (SD) ( $n = 3$ ). (TIF)

**S14 Fig. *S. chromogenes* and *Av. paragallinarum* invade respiratory host cells.** (A) Confocal images of internalized bacteria in epithelial cells. A549 cells were infected with pHrodoRed-labeled *Av. paragallinarum* X1-1S-1 or *S. chromogenes* SC10 (MOI = 20) for 1 h. F-actin was stained with ActinGreen 488 ReadyProbes (green), and the nuclei were counterstained with DAPI (blue). Scale bar = 10  $\mu\text{m}$ . (B) The numbers of internalized *S. chromogenes* and *Av. paragallinarum* were measured by the gentamycin protection assay after the mono-infection or coinfection of these two bacteria (MOI = 1) for 6 h. (C) Merged exhibition of the extracellular and intracellular numbers of *Av. paragallinarum* from (B), Figs 6A and S10B. (D) Ratio of extracellular/intracellular *Av. paragallinarum* from (C). (E) Ratio of *Av. paragallinarum* in experimental groups of coinfection/mono-infection from (C). *P* values were determined by unpaired *t*-test. The mean of three biological replicates is shown, and error bars represent the standard deviation (SD) ( $n = 3$ ). (TIF)

## Author Contributions

**Conceptualization:** Guozhong Zhang, Kui Zhu.

**Data curation:** Yifan Wu, Yongqiang Wang, Qian Li.

**Formal analysis:** Huiming Yang.

**Funding acquisition:** Guozhong Zhang, Kui Zhu.

**Investigation:** Yifan Wu, Qian Li, Xiaoxia Gong, Kui Zhu.

**Methodology:** Yifan Wu.

**Project administration:** Guozhong Zhang, Kui Zhu.

**Resources:** Yongqiang Wang.

**Software:** Yifan Wu.

**Supervision:** Guozhong Zhang, Kui Zhu.

**Validation:** Yifan Wu, Huiming Yang, Xiaoxia Gong, Kui Zhu.

**Visualization:** Yifan Wu, Kui Zhu.

**Writing – original draft:** Yifan Wu, Kui Zhu.

**Writing – review & editing:** Yifan Wu, Kui Zhu.

## References

1. Kamada N, Nunez G. Regulation of the immune system by the resident intestinal bacteria. *Gastroenterology*. 2014; 146(6):1477–88. <https://doi.org/10.1053/j.gastro.2014.01.060> PMID: 24503128
2. Man WH, de Steenhuijsen Piters WA, Bogaert D. The microbiota of the respiratory tract: gatekeeper to respiratory health. *Nat Rev Microbiol*. 2017; 15(5):259–70. <https://doi.org/10.1038/nrmicro.2017.14> PMID: 28316330
3. Baumler AJ, Sperandio V. Interactions between the microbiota and pathogenic bacteria in the gut. *Nature*. 2016; 535(7610):85–93. <https://doi.org/10.1038/nature18849> PMID: 27383983
4. Perez-Lopez A, Behnsen J, Nuccio S-P, Raffatellu M. Mucosal immunity to pathogenic intestinal bacteria. *Nat Rev Immunol*. 2016; 16(3):135–48. <https://doi.org/10.1038/nri.2015.17> PMID: 26898110
5. Cohen TS, Hilliard JJ, Jones-Nelson O, Keller AE, O'Day T, Tkaczyk C, et al. *Staphylococcus aureus* alpha toxin potentiates opportunistic bacterial lung infections. *Sci Transl Med*. 2016; 8(329):329ra31. <https://doi.org/10.1126/scitranslmed.aad9922> PMID: 26962155
6. Abt MC, McKenney PT, Pamer EG. Clostridium difficile colitis: pathogenesis and host defence. *Nat Rev Microbiol*. 2016; 14(10):609–20. <https://doi.org/10.1038/nrmicro.2016.108> PMID: 27573580
7. Molyneaux PL, Mallia P, Cox MJ, Footitt J, Willis-Owen SA, Homola D, et al. Outgrowth of the bacterial airway microbiome after rhinovirus exacerbation of chronic obstructive pulmonary disease. *Am J Respir Crit Care Med*. 2013; 188(10):1224–31. <https://doi.org/10.1164/rccm.201302-0341OC> PMID: 23992479
8. Arike L, Hansson GC. The densely O-glycosylated MUC2 mucin protects the intestine and provides food for the commensal bacteria. *J Mol Biol*. 2016; 428(16):3221–9. <https://doi.org/10.1016/j.jmb.2016.02.010> PMID: 26880333
9. EL B. Our understanding of the Pasteurellaceae. *Can J Vet Res*. 1990; 54:S78–82. PMID: 2193710
10. Inzana TJ, Clarridge J, Williams RP. Rapid determination of X/V growth requirements of Haemophilus species in broth. *Diagn Microbiol Infect Dis*. 1987; 6(2):93–100. [https://doi.org/10.1016/0732-8893\(87\)90092-7](https://doi.org/10.1016/0732-8893(87)90092-7) PMID: 3493113
11. O'Reilly T, Niven DF. Levels of nicotinamide adenine dinucleotide in extracellular body fluids of pigs may be growth-limiting for Actinobacillus pleuropneumoniae and Haemophilus parasuis. *Can J Vet Res*. 2003; 67(3):229–31. PMID: 12889731
12. Clement J, Wong M, Poljak A, Sachdev P, Braidy N. The Plasma NAD(+) Metabolome Is Dysregulated in "Normal" Aging. *Rejuvenation Res*. 2019; 22(2):121–30. <https://doi.org/10.1089/rej.2018.2077> PMID: 30124109

13. Houtkooper RH, Canto C, Wanders RJ, Auwerx J. The secret life of NAD<sup>+</sup>: an old metabolite controlling new metabolic signaling pathways. *Endocr Rev.* 2010; 31(2):194–223. <https://doi.org/10.1210/er.2009-0026> PMID: 20007326
14. Haag F, Adriouch S, Brass A, Jung C, Moller S, Scheuplein F, et al. Extracellular NAD and ATP: Partners in immune cell modulation. *Purinergic Signal.* 2007; 3(1–2):71–81. <https://doi.org/10.1007/s11302-006-9038-7> PMID: 18404420
15. Long JS, Mistry B, Haslam SM, Barclay WS. Host and viral determinants of influenza A virus species specificity. *Nat Rev Microbiol.* 2019; 17(2):67–81. <https://doi.org/10.1038/s41579-018-0115-z> PMID: 30487536
16. Cechova L, Halanova M, Babinska I, Danisova O, Bartkovsky M, Marcincak S, et al. Chlamydiosis in farmed chickens in Slovakia and zoonotic risk for humans. *Ann Agric Environ Med.* 2018; 25(2):320–5. <https://doi.org/10.26444/aaem/82948> PMID: 29936804
17. Sollid JU, Furberg AS, Hanssen AM, Johannessen M. *Staphylococcus aureus*: determinants of human carriage. *Infect Genet Evol.* 2014; 21:531–41. <https://doi.org/10.1016/j.meegid.2013.03.020> PMID: 23619097
18. Chanteloup NK, Porcheron G, Delaleu B, Germon P, Schouler C, Moulin-Schouleur M, et al. The extra-intestinal avian pathogenic *Escherichia coli* strain BEN2908 invades avian and human epithelial cells and survives intracellularly. *Vet Microbiol.* 2011; 147(3–4):435–9. <https://doi.org/10.1016/j.vetmic.2010.07.013> PMID: 20708353
19. EG. H. Some characteristics of *Staphylococcus aureus* isolated from the skin and upper respiratory tract of domesticated and wild (Feral) birds. *Res Vet Sci.* 1967; 8(4):490–9. PMID: 5183295
20. Foley SL, Johnson TJ, Ricke SC, Nayak R, Danzeisen J. *Salmonella* pathogenicity and host adaptation in chicken-associated serovars. *Microbiol Mol Biol Rev.* 2013; 77(4):582–607. <https://doi.org/10.1128/MMBR.00015-13> PMID: 24296573
21. Blackall PJ, Soriano-Vargas E. Infectious coryza and related bacterial infections. In: Swayne D.E., Glisson J.R., McDougald L.R., Nolan L.K., Suarez D.L., Nair V.L. (Eds.). *Diseases of Poultry.* 2013; 13th ed. John Wiley & Sons, Inc., Ames, IA, USA, pp:859–68.
22. Blackall PJ. Infectious coryza: overview of the disease and new diagnostic options. *Clin Microbiol Rev.* 1999; 12(4):627–32. PMID: 10515906
23. Pickett MJ, Stewart RM. Identification of hemophilic bacilli by means of the satellite phenomenon. *Am J Clin Pathol.* 1953; 23(7):713–5. <https://doi.org/10.1093/ajcp/23.7.ts.713> PMID: 13080211
24. Casteleyn C, Cornillie P, Van Cruchten S, Van den Broeck W, Van Ginneken C, Simoens P. Anatomy of the upper respiratory tract in domestic birds, with emphasis on vocalization. *Anat Histol Embryol.* 2018; 47(2):100–9. <https://doi.org/10.1111/ahc.12336> PMID: 29322535
25. Sakamoto R, Kino Y, Sakaguchi M. Development of a multiplex PCR and PCR-RFLP method for serotyping of *Avibacterium paragallinarum*. *J Vet Med Sci.* 2012; 74(2):271–3. <https://doi.org/10.1292/jvms.11-0319> PMID: 21979456
26. Xu Y, Cheng J, Huang X, Xu M, Feng J, Liu C, et al. Characterization of emergent *Avibacterium paragallinarum* strains and the protection conferred by infectious coryza vaccines against them in China. *Poult Sci.* 2019; 98(12):6463–71. <https://doi.org/10.3382/ps/pez531> PMID: 31801310
27. Mei C, Xian H, Blackall PJ, Hu W, Zhang X, Wang H. Concurrent infection of *Avibacterium paragallinarum* and fowl adenovirus in layer chickens. *Poult Sci.* 2020; 99(12):6525–32. <https://doi.org/10.1016/j.psj.2020.09.033> PMID: 33248567
28. Zhang Z, Adappa ND, Lautenbach E, Chiu AG, Doghramji LJ, Cohen NA, et al. Coagulase-negative *Staphylococcus* culture in chronic rhinosinusitis. *Int Forum Allergy Rhinol.* 2015; 5(3):204–13. <https://doi.org/10.1002/alr.21439> PMID: 25367456
29. Avall-Jaaskelainen S, Taponen S, Kant R, Paulin L, Blom J, Palva A, et al. Comparative genome analysis of 24 bovine-associated *Staphylococcus* isolates with special focus on the putative virulence genes. *PeerJ.* 2018; 6:e4560. <https://doi.org/10.7717/peerj.4560> PMID: 29610707
30. Ruiz-Romero RA, Cervantes-Olivares RA, Ducoing-Watty AE, Martinez-Gomez D, Diaz-Aparicio E, Mendez-Olvera ET. Genetic analysis method for *Staphylococcus chromogenes* associated with goat mastitis. *Pol J Microbiol.* 2018; 67(2):171–80. <https://doi.org/10.21307/pjm-2018-019> PMID: 30015455
31. Slack MPE. 31—*Haemophilus*: Respiratory infections; meningitis; chancroid. D. Greenwood MB, Slack R., Irving W., editor. Churchill Livingstone.2012. 324–30 p.
32. Zhang P, Zhang C, Aragon V, Zhou X, Zou M, Wu C, et al. Investigation of *Haemophilus parasuis* from healthy pigs in China. *Vet Microbiol.* 2019; 231:40–4. <https://doi.org/10.1016/j.vetmic.2019.02.034> PMID: 30955821
33. Tsuji A, Maeda M, Arakawa H. Chemiluminescent assay of co-factors. *J Biolumin Chemilumin.* 1989; 4(1):454–62. <https://doi.org/10.1002/bio.1170040160> PMID: 2801232

34. Paudel S, Hess M, Hess C. Coinfection of *Avibacterium paragallinarum* and *Gallibacterium anatis* in specific-pathogen-free chickens complicates clinical signs of infectious coryza, which can be prevented by vaccination. *Avian Dis.* 2017; 61(1):55–63. <https://doi.org/10.1637/11481-081016-Reg> PMID: 28301236
35. Morales-Erasto V, Falconi-Agapito F, Luna-Galaz GA, Saravia LE, Montalvan-Avalos A, Soriano-Vargas EE, et al. Coinfection of *Avibacterium paragallinarum* and *Ornithobacterium rhinotracheale* in Chickens from Peru. *Avian Dis.* 2016; 60(1):75–8. <https://doi.org/10.1637/11265-082015-ResNote.1> PMID: 26953948
36. De Buhr N, Bonilla MC, Pfeiffer J, Akhdar S, Schwennen C, Kahl BC, et al. Degraded neutrophil extracellular traps promote the growth of *Actinobacillus pleuropneumoniae*. *Cell Death Dis.* 2019; 10(9):657. <https://doi.org/10.1038/s41419-019-1895-4> PMID: 31506432
37. Chiarugi A, Dolle C, Felici R, Ziegler M. The NAD metabolome—a key determinant of cancer cell biology. *Nat Rev Cancer.* 2012; 12(11):741–52. <https://doi.org/10.1038/nrc3340> PMID: 23018234
38. Pajuelo D, Gonzalez-Juarbe N, Tak U, Sun J, Orihuela CJ, Niederweis M. NAD(+) Depletion triggers macrophage necroptosis, a cell death pathway exploited by *Mycobacterium tuberculosis*. *Cell Rep.* 2018; 24(2):429–40. <https://doi.org/10.1016/j.celrep.2018.06.042> PMID: 29996103
39. Cea M, Cagnetta A, Fulciniti M, Tai YT, Hideshima T, Chauhan D, et al. Targeting NAD<sup>+</sup> salvage pathway induces autophagy in multiple myeloma cells via mTORC1 and extracellular signal-regulated kinase (ERK1/2) inhibition. *Blood.* 2012; 120(17):3519–29. <https://doi.org/10.1182/blood-2012-03-416776> PMID: 22955917
40. Ueda S, Nagasawa Y, Suzuki T, Tajima M. Adhesion of *Haemophilus paragallinarum* to cultured chicken cells. *Microbiol Immunol.* 1982; 26(11):1007–16. <https://doi.org/10.1111/j.1348-0421.1982.tb00250.x> PMID: 7167062
41. Hardison RL, Heimlich DR, Harrison A, Beatty WL, Rains S, Moseley MA, et al. Transient nutrient deprivation promotes macropinocytosis-dependent intracellular bacterial community development. *mSphere.* 2018; 3(5).
42. Liu X, Liu F, Ding S, Shen J, Zhu K. Sublethal levels of antibiotics promote bacterial persistence in epithelial cells. *Adv Sci (Weinh).* 2020; 7(18):1900840. <https://doi.org/10.1002/advs.201900840> PMID: 32999821
43. Norskov-Lauritsen N. Classification, identification, and clinical significance of *Haemophilus* and *Aggregatibacter* species with host specificity for humans. *Clin Microbiol Rev.* 2014; 27(2):214–40. <https://doi.org/10.1128/CMR.00103-13> PMID: 24696434
44. Niven DF, O'Reilly T. Significance of V-factor dependency in the taxonomy of *Haemophilus* species and related organisms. *Int J Syst Bacteriol.* 1990; 40(1):1–4. <https://doi.org/10.1099/00207713-40-1-1> PMID: 2145965
45. Margolis E, Yates A, Levin BR. The ecology of nasal colonization of *Streptococcus pneumoniae*, *Haemophilus influenzae* and *Staphylococcus aureus*: the role of competition and interactions with host's immune response. *BMC Microbiol.* 2010; 10:59. <https://doi.org/10.1186/1471-2180-10-59> PMID: 20178591
46. Shiri T, Nunes MC, Adrian PV, Van Niekerk N, Klugman KP, Madhi SA. Interrelationship of *Streptococcus pneumoniae*, *Haemophilus influenzae* and *Staphylococcus aureus* colonization within and between pneumococcal-vaccine naive mother-child dyads. *BMC Infect Dis.* 2013; 13:483. <https://doi.org/10.1186/1471-2334-13-483> PMID: 24134472
47. Ashrafi R, Bruneaux M, Sundberg LR, Pulkkinen K, Valkonen J, Ketola T. Broad thermal tolerance is negatively correlated with virulence in an opportunistic bacterial pathogen. *Evol Appl.* 2018; 11(9):1700–14. <https://doi.org/10.1111/eva.12673> PMID: 30344637
48. Chen P, Shakhnovich EI. Thermal adaptation of viruses and bacteria. *Biophys J.* 2010; 98(7):1109–18. <https://doi.org/10.1016/j.bpj.2009.11.048> PMID: 20371310
49. Salaberry SR, Saldenberger AB, Zuniga E, Melville PA, Santos FG, Guimaraes EC, et al. Virulence factors genes of *Staphylococcus* spp. isolated from caprine subclinical mastitis. *Microb Pathog.* 2015; 85:35–9. <https://doi.org/10.1016/j.micpath.2015.05.007> PMID: 26026835
50. Shen Y, Zhou H, Xu J, Wang Y, Zhang Q, Walsh TR, et al. Anthropogenic and environmental factors associated with high incidence of *mcr-1* carriage in humans across China. *Nat Microbiol.* 2018; 3(9):1054–62. <https://doi.org/10.1038/s41564-018-0205-8> PMID: 30038311
51. CLSI. Performance Standards for Antimicrobial Disk and Dilution Susceptibility Tests for Bacteria Isolated from Animals: 4th ed. 2018; CLSI supplement VET08. Wayne, PA, USA.
52. CLSI. Clinical and Laboratory Standards Institute. Performance Standards for Antimicrobial Susceptibility Testing: 28th ed. 2018; CLSI supplement M100. Wayne, PA, USA.

53. Liu Y, Ding S, Dietrich R, Martlbauer E, Zhu K. A biosurfactant-inspired heptapeptide with improved specificity to kill MRSA. *Angew Chem Int Ed Engl*. 2017; 56(6):1486–90. <https://doi.org/10.1002/anie.201609277> PMID: 28106348
54. Song M, Liu Y, Huang X, Ding S, Wang Y, Shen J, et al. A broad-spectrum antibiotic adjuvant reverses multidrug-resistant Gram-negative pathogens. *Nat Microbiol*. 2020. <https://doi.org/10.1038/s41564-020-0723-z> PMID: 32424338
55. Wu Y, Fan R, Wang Y, Lei L, Fessler AT, Wang Z, et al. Analysis of combined resistance to oxazolidinones and phenicols among bacteria from dogs fed with raw meat/vegetables and the respective food items. *Sci Rep*. 2019; 9(1):15500. <https://doi.org/10.1038/s41598-019-51918-y> PMID: 31664106
56. Kong X, Yu S, Fang W, Liu J, Li H. Enhancing syntrophic associations among *Clostridium butyricum*, *Syntrophomonas* and two types of methanogen by zero valent iron in an anaerobic assay with a high organic loading. *Bioresour Technol*. 2018; 257:181–91. <https://doi.org/10.1016/j.biortech.2018.02.088> PMID: 29501951
57. Bolger A, Lohse M, Usadel B. Trimmomatic: A flexible read trimming tool for Illumina NGS data. *Bioinformatics*. 2014; 30(15):2114–20. <https://doi.org/10.1093/bioinformatics/btu170> PMID: 24695404
58. Edgar RC, Flyvbjerg H. Error filtering, pair assembly and error correction for next-generation sequencing reads. *Bioinformatics*. 2015; 31(21):3476–82. <https://doi.org/10.1093/bioinformatics/btv401> PMID: 26139637
59. Edgar RC. UPARSE: highly accurate OTU sequences from microbial amplicon reads. *Nat Methods*. 2013; 10(10):996–8. <https://doi.org/10.1038/nmeth.2604> PMID: 23955772
60. Chowdhry S, Zanca C, Rajkumar U, Koga T, Diao Y, Raviram R, et al. NAD metabolic dependency in cancer is shaped by gene amplification and enhancer remodelling. *Nature*. 2019; 569(7757):570–5. <https://doi.org/10.1038/s41586-019-1150-2> PMID: 31019297
61. Hara N, Yamada K, Shibata T, Osago H, Hashimoto T, Tsuchiya M. Elevation of cellular NAD levels by nicotinic acid and involvement of nicotinic acid phosphoribosyltransferase in human cells. *J Biol Chem*. 2007; 282(34):24574–82. <https://doi.org/10.1074/jbc.M610357200> PMID: 17604275
62. Chang HC, Guarente L. SIRT1 mediates central circadian control in the SCN by a mechanism that decays with aging. *Cell*. 2013; 153(7):1448–60. <https://doi.org/10.1016/j.cell.2013.05.027> PMID: 23791176
63. Habeichi NJ, Mroueh A, Kaplan A, Ghali R, Al-Awassi H, Tannous C, et al. Sex-based differences in myocardial infarction-induced kidney damage following cigarette smoking exposure: more renal protection in premenopausal female mice. *Biosci Rep*. 2020; 40(6). <https://doi.org/10.1042/BSR20193229> PMID: 32519752
64. Kuribayashi H, Baba Y, Iwagawa T, Arai E, Murakami A, Watanabe S. Roles of Nmnat1 in the survival of retinal progenitors through the regulation of pro-apoptotic gene expression via histone acetylation. *Cell Death Dis*. 2018; 9(9):891. <https://doi.org/10.1038/s41419-018-0907-0> PMID: 30166529
65. Song T, Yang L, Kabra N, Chen L, Koomen J, Haura EB, et al. The NAD<sup>+</sup> synthesis enzyme nicotinamide mononucleotide adenylyltransferase (NMNAT1) regulates ribosomal RNA transcription. *J Biol Chem*. 2013; 288(29):20908–17. <https://doi.org/10.1074/jbc.M113.470302> PMID: 23737528
66. Augustyniak J, Lenart J, Lipka G, Stepien PP, Buzanska L. Reference Gene Validation via RT-qPCR for Human iPSC-Derived Neural Stem Cells and Neural Progenitors. *Mol Neurobiol*. 2019; 56(10):6820–32. <https://doi.org/10.1007/s12035-019-1538-x> PMID: 30927132
67. Arzanlou M, Chai WC, Venter H. Intrinsic, adaptive and acquired antimicrobial resistance in Gram-negative bacteria. *Essays Biochem*. 2017; 61(1):49–59. <https://doi.org/10.1042/EBC20160063> PMID: 28258229
68. Michael GB, Bosse JT, Schwarz S. Antimicrobial Resistance in *Pasteurellaceae* of Veterinary Origin. *Microbiol Spectr*. 2018; 6(3). <https://doi.org/10.1128/microbiolspec.ARBA-0022-2017> PMID: 29916344